Water Air Soil Pollut (2023) 234:136
https://doi.org/10.1007/s11270-023-06146-6

Specific Surface Area Versus Adsorptive Capacity: an Application View of 3D Graphene-Based Materials for the Removal of Emerging Water Pollutants

Mayara Bitencourt Leão · José Rafael Bordin · Carolina Ferreira de Matos

Received: 9 September 2022 / Accepted: 1 February 2023 / Published online: 15 February 2023

Abstract Three-dimensional graphene-based materials have emerged as adsorbents for various contaminants. This property is usually attributed to its high surface area. However, studies showing a positive correlation between surface area versus adsorptive capacity are not found in the literature. This review summarizes recent studies involving different types of adsorbents based on 3D graphene (including pure 3D graphene and composites) from the angle of experimental parameters such as contact time, adsorbent dosage, pH, and initial concentration. A particular focus is given to the correlation of their adsorption efficiency characteristics from the specific surface area, demonstrating that this parameter is not essential to obtaining good adsorption results. Furthermore, we will discuss their applications in removing various emerging pollutants from water (drugs, pesticides, hydrocarbons, organic solvents, endocrine disruptors), oils, dyes, and heavy metal ions, correlating fundamental properties of 3D materials with their efficiency. Finally, the challenges and perspectives of 3D graphene-based materials will be pointed out. Hopefully, this review will help design efficient 3D graphene adsorbents for pollutant removal.

Keywords Adsorption · Nanomaterials · Emerging contaminants · Three-dimensional graphene

M. B. Leão · C. F. de Matos (✉)
Environmental Science and Technology Center, Universidade Federal Do Pampa, Campus Caçapava Do Sul, Caçapava Do Sul, RS 96570-000, Brazil
e-mail: carolinamatos@unipampa.edu.br

J. R. Bordin
Department of Physics, Institute of Physics and Mathematics, Universidade Federal de Pelotas, Capão Do Leão, RS 96050-500, Brazil

1 Introduction

Undoubtedly, one of the great challenges of our scientific generation is to find out alternatives to water scarcity. Nowadays, the huge imbalance between clean water demand and total supply makes freshwater resources dry up unprecedentedly (Unesco, 2019). As a consequence, nearly half of the world population suffers from water stress, and these numbers will worsen in the following decades due to population growth, climate change, political decisions, and our current lifestyle (Eliasson, 2015). Therefore, fixing this imbalance is a scientific task and reflects environmental, geopolitical, and humanitarian aspects.

Human negligence with the water supplies becomes evident since 80% of residuals water, from industry to city sewers, returns to water bodies without the proper treatment. The consequence is the increasing contamination and degradation of aqueous environments, which leads to water scarcity and health issues related to contaminated water. The low-income population is the most affected, leading to even lower human dignity for this population

(Unesco, 2017). Our role as scientists is to seek technological outcomes to overcome this issue. Therefore, efforts have been made to find better, cheaper, and greener structures for water cleaning. Various methods have been employed: screening, filtration, centrifugation, crystallization, sedimentation and separation by gravity, flotation, precipitation, coagulation, oxidation, solvent extraction, evaporation, distillation, reverse osmosis, ion exchange, electrodialysis, electrolysis, and adsorption (Ali et al., 2018). This variety of methods employs the most different types of materials. However, most materials cannot remove a large variety of pollutants, especially at natural water pH or contaminant trace level concentration (Ali et al., 2015; Solangi et al., 2021).

In this direction, one of the huge tasks in the current materials science is to develop a material able to adsorb a broad spectrum of water pollutants (Chen et al., 2013a). Among the several materials proposed in recent years, carbon-based and graphene-based nanostructures are among the most prominent water purification technologies (Köhler et al., 2019a, 2021; Mauter & Elimelech, 2008). This applicability is directly related to impressive graphene properties, such as mechanical flexibility, chemical and thermal stability, and high surface area (Allen et al., 2010; Geim, 2009; Rao et al., 2009; Stoller et al., 2008). Nevertheless, when pristine graphene is used as an adsorbent, the main interaction with the contaminants comes from the van der Walls forces related to the sp^2 carbon. Consequently, polar pollutants, like heavy metals, prefer to remain in the bulk water instead of adsorbing on the graphene surface (Köhler et al., 2018, 2019b). A way to overcome this is to add to the graphene materials or molecules with specific functional groups, leading to better adsorbent properties (Velusamy et al., 2021), thereby improving the number of possible applications of graphene-based materials for water treatment (Asghar et al., 2022; Asif et al., 2021), including dye removal (Majumder & Gangopadhyay, 2022; Yap et al., 2021), organic solvents (Yap et al., 2021), pesticides (Power et al., 2018; Yang et al., 2021), heavy metals (Abu-Nada et al., 2020; Lim et al., 2018; Xu et al., 2018a, b), and other inorganic pollutants (Verma & Nadagouda, 2021).

3D graphene (3D-G) based macrostructures have shown high adsorption capacity and huge recyclability due to their unique superficial area and porosity (Chen et al., 2013a, b, c; Yousefi et al., 2019). Briefly stated, 3D-G multifunctional structures are obtained by employing methods that prevent the graphene sheets from stacking in the suspended solution. This 3D configuration keeps the graphene sheet properties and increases applications based on characteristics that single sheets do not have as porosity. Several studies have been dedicated to synthesizing 3D-G structures with distinct morphology, structures, and properties (Cao et al., 2014). Typical 3D-G structures include graphene foam, graphene sponges, and graphene aerogels (Chen et al., 2011), and they have physical–chemical properties that diverge from the chemical building blocks—the pristine graphene and the functionalization molecules. The 3D architecture prevents spontaneous self-assembly in water (Mauter & Elimelech, 2008; Sun et al., 2020), leading to high stability in aqueous solutions (Yu et al., 2013). 3D-G also is highly stable in distinct aqueous environments, from saltwater to mixtures of water and nitric acid, and even in organic solvents, such as dimethylformamide and cyclohexane (Wang et al., 2013). This stable structure allows this type of material to present less toxicity when compared to other graphene species (da Rosa et al., 2021; Leão et al., 2022). Micro-sized pollutants, like tetracycline, chlorophenols, or fluorides, have also been adsorbed with high efficiency (Chen et al., 2013b; Liu et al., 2014; Zhao et al., 2013).

Besides pristine graphene, graphene oxide (GO) has attracted attention for water decontamination due to its properties at the natural aqueous pH levels and its high efficiency in removing pollutants at low concentrations (Ali et al., 2018). Also, GO shows good electronic mobility, high thermal conductivity, and remarkable mechanical strength. Recent studies indicate that GO sheets can be synthesized on a large scale by graphite exfoliation (Smith et al., 2019), easily leading to industrial-level production. Its surface can be easily functionalized by the strong π–π stacking and van der Waals interactions (Ma & Zhi, 2021). Nonetheless, the GO suspended solution can be reordered to create self-assembled 2D or 3D structures (Smith et al., 2019). Therefore, 3D-GO structures have also arisen as promising new materials for new technologies for water cleaning.

In previously published works, literature reviews were carried out using three-dimensional graphene-based materials for water purification. One of the first works in this direction was published in 2015 and evaluated the elimination of oil particles from water

through adsorption (Wong et al., 2022) . In the same year, a complete work was published describing the applications and environmental mechanisms of 3D graphene materials. "Structure-ownership-application" relationships were established, and although complete, this review can already be considered outdated (Shen et al., 2015). In 2018, a review focused on methods of synthesizing 3D graphene-based structures and evaluating their adsorption performance of dyes, heavy metals, and pharmaceuticals. This work verified that its adsorptive properties were influenced by pollutant characteristics, adsorbent surface, and process parameters (Hiew et al., 2018). In 2019, a review summarized the environmental and self-assembly applications of 3D graphene-based materials in removing contaminants from water and air. The surface areas were compared with other materials, but in general and without details (Yousefi et al., 2019). Three more reviews were published the following year, focusing on removing contaminants from wastewater (Bano et al., 2020), an overview of the applications of 3D graphene in water purification without much detail (Wang et al., 2019a, b), and the view of adsorbents and their functionalization in the removal of pollutants from water. In this work, a great focus was given to detailing the synthesis processes, and adsorption was briefly discussed (Liu & Qiu, 2020). Finally, in 2021, a review was made available that evaluated the modification strategies and performances of modified 3D graphene materials to remove residual gases, refractory organics, and heavy metals (Lin et al., 2021). Although many reviews of three-dimensional graphene-based materials have been published to date, no review clearly highlights the influence of specific surface area on the adsorption process. In this context, this review presents a systematic review of 3D graphene-based materials and their applications for water treatment, relating the adsorption results to the specific surface areas of each material.

In this context, this review presents a systematic review of 3D graphene-based materials and their applications for water treatment. First, Section 2 discusses the distinct morphology observed in hierarchical 3D graphene structures and their individual properties. Next, we review the considerable number of new applications for pollutant removal. In Section 3, we show the applications for pesticide removal. Section 4 is dedicated to discussing the efforts to separate water and drugs, while in Section 5, we show the recent advances to remove other emerging contaminants; in Section 6, heavy metals, and in Section 7, we discuss the removal of dyes. The possible mechanisms of adsorption of contaminants in 3D graphene are presented in Section 8, and finally, our conclusions and perspectives are shown in Section 9.

2 3D Graphene-Based Materials

The scientific and technological possibilities of carbon-based nanostructures became notorious after the work by Iijima (1991), which reported the fabrication of carbon nanotubes (CNT) and started the "boom" in this area. The idea of 3D structures based on carbon is even earlier than the seminal works where Novoselov et al. (2004) reported the isolation of graphene sheets. The hypothesis of hierarchical self-assembly of carbon foams from nanostructured graphite was made by Umemoto and co-workers (2001) 3 years early. However, the mechanical exfoliation method of Novoselov and Geim is one of the greatest revolutions in the Chemical, Physical, and Engineering Sciences of our Century.

Spontaneous self-assembly is one of the most prominent and efficient strategies for building macroscopic structures from nanosized chemical building blocks (Jing et al., 2022). It allows us to explore the unique properties of nanomaterials in macroscopic devices (Tang et al., 2010; Xu & Shi, 2011), and the unique properties and versatility of carbon-based nanomaterials make them the best candidates for self-assembled materials. In the carbon allotrope-based materials, the first CNT-based 3D aerogels were reported in Bryning et al., 2007 by Bryning and co-authors and in Worsley et al., 2008 by Worsley and co-authors. After, two distinct groups obtained graphene-based aerogels by lyophilization in 2009 (Vickery et al., 2009; Wang & Ellsworth, 2009). After that, many other self-assembled macrostructures based on graphene were reported in the literature. Distinct methods can lead to specific characteristics and properties, such as low density, high porosity, large specific surface area, superhydrophobic surfaces, great mechanical resistance, and high electrochemical performance (Lee et al., 2015; Shan et al., 2018; Sun et al., 2016; Yousefi et al., 2019; Zarbin & Oliveira, 2013). The assembly of 3D-G structures presents one

of the most promising strategies in nanoscience and nanotechnology (Nardecchia et al., 2013) and controls the synthesis, if possible, to control the obtained morphology (Leão et al., 2022). We can divide the morphologies between two families: the hollow nanostructures and the porous structures. Hollow structures include graphene nanoshells (Bachmatiuk et al., 2013; Peng et al., 2013, 2014), shown in Fig. 1a, graphene nanospheres (Yoon et al., 2012), Fig. 1b, carbon nanococoons (Zhang et al., 2014), Fig. 1c, and carbon capsules (Kim et al., 2011), Fig. 1d. Porous structures can be graphene aerogels (Hu et al., 2013; Ji et al., 2013), as we show in Fig. 1e, or graphene sponges (Bong et al., 2015; Chen et al., 2011; Xu et al., 2010), exemplified in Fig. 1f.

The porous structures are the most relevant for adsorption due to their high surface area. Aerogels are 3D structures with a low density, high surface area, and high porosity synthesized from a gel in which a gas replaces the dispersion liquid. These characteristics facilitate functionalization, and several studies have explored this feature (Fang & Chen, 2014; Zhang et al., 2014, 2015a, b). As an example, Ji et al. (2013) explored the use of three different carbohydrates. Their results showed that distinct structures were obtained by changing the carbohydrate type. Then, it is possible to control the morphology by changing the reducing and spacer agents, which can be extended to other materials.

Graphene sponges are also light and porous, with a morphology created by introducing gas bubbles in the production process. It consists of an interconnected flexible network with excellent porosity and electrical conductivity. In this sense, a hydrothermal method can be used to grow a self-assembled graphene sponge. This 3D-G structure shows excellent thermal and mechanical stability, high electrical conductance, high specific capacity, and exciting biotechnology and electrochemistry applications (Beitollai et al., 2019). Besides, 3D-G structures can be functionalized with several materials, such as metallic nanoparticles (Lee et al., 2015), sugar (Bose & Drzal, 2015), polyelectrolytes (Qi et al., 2010), biomolecules (Passaretti, 2022), and

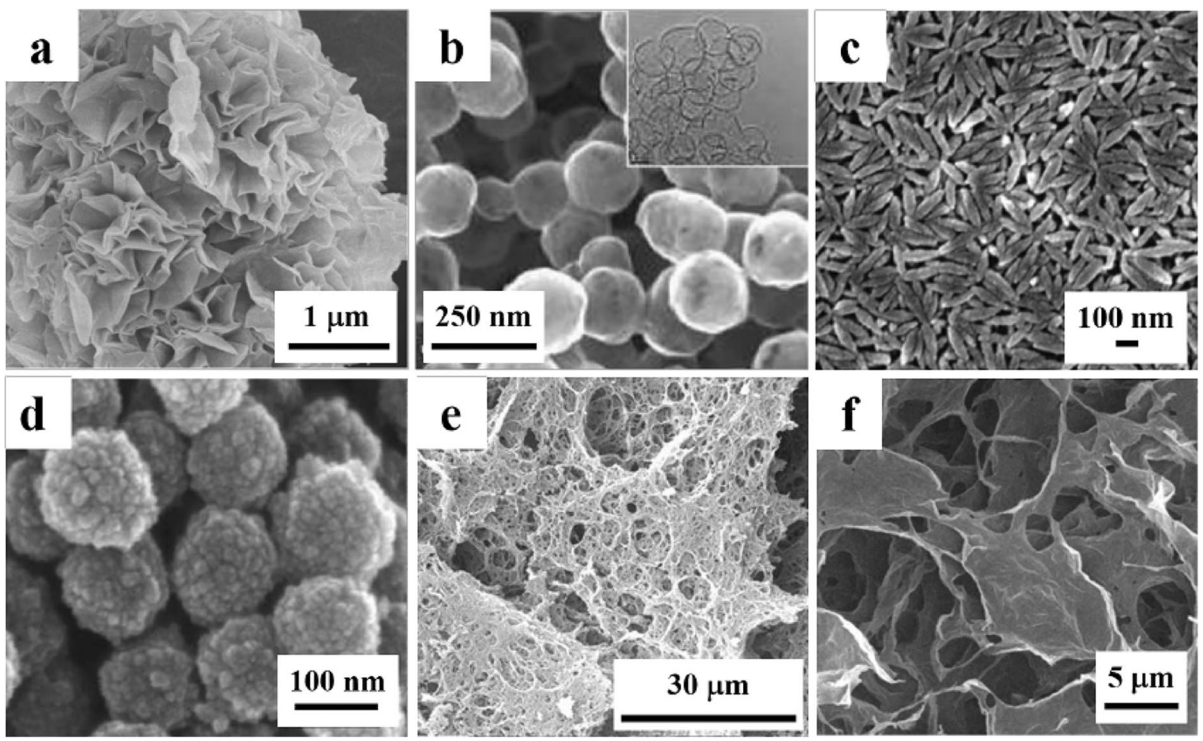

Fig. 1 SEM images of **a** graphene nanoshells, adapted from Peng et al. (2014); **b** graphene nanospheres, adapted from Yoon et al. (2012); **c** carbon nanococoons, adapted from Zhang et al. (2014); **d** carbon capsules, adapted from Kim et al. (2011); **e** graphene aerogels, adapted from Ji et al. (2013), and **f** graphene sponges, adapted from Xu et al. (2010)

more. Each chemical functionalization and each specific structure led to specific adsorption properties—whose applications will be discussed in the following sections.

Despite its exceptional properties and promising applications, reducing agents are a significant problem in graphene-based materials synthesis. Most chemical reactants employed to reduce the graphene oxide sheets into a 3D structure are toxic. For instance, one of the most used reducing agents is hydrazine (N_2H_4) (Oliveira et al., 2015). It has an excellent reducing capacity but may have hemotoxicity, hepatotoxicity, neurotoxicity, lung lesions, and skin irritations (Nguyen et al., 2021). Another reducing agent widely applied in 3D-G synthesis is sodium borohydride ($NaBH_4$) (Feng et al., 2020). Unfortunately, this compound is highly toxic to the environment. Nonetheless, it is toxic if swallowed, and when in contact with the skin and, when in contact with water, the reaction releases gases that can spontaneously ignite (Brasileira, 2017). More recently, some synthesis methods developed use natural reducing agents, such as ascorbic acid, which can solve the problems related to the reagents above (Leão et al., 2022).

Another problem is the time required for the synthesis. In the current methods (Chen et al., 2014a, b; Fang et al., 2017; Gao et al., 2013; Ma et al., 2015; Shan et al., 2018), the number of steps and the time required are huge, taking several days—or weeks—to get a sample, with a few exceptions found (Leão et al., 2022). Besides that, in some cases, templates, such as low-viscosity polymers (Guan et al., 2018), nickel foam (Chen et al., 2014a, b), epoxy resin (Jia et al., 2014, and calcium carbonate ($CaCO_3$) (Meng et al., 2013), have to been employed to create the 3D-G structures.

Therefore, those are relevant problems to be concerned about: there is no point in trying to clean water by polluting water, and the production is cheap, with few steps and no templates. Therefore, it is necessary to create new chemical routines to obtain 3D-G macrostructures, employing non-pollutant reducing agents and speeding the process to achieve sizeable industrial production. From now on, we will present a synthesis of the works carried out in recent years using three-dimensional graphene materials to remove contaminants from water.

3 Pesticides

Pesticides are chemicals employed mainly in plantations, from small to large crops of practically all the food consumed worldwide. Most pesticides are natural or synthetic xenobiotics, with toxic activity employed to control or eradicate crop plagues and diseases (Kong et al., 2021b). Although it has an essential role in the food industry, the incorrect misuse and disposal of pesticides can lead to sanitary, environmental (Leão et al., 2019; Rani et al., 2021; Siviter et al., 2021; Tang et al., 2021), and health (Rani et al., 2021) issues. It is a consequence of the fact that pesticides are resistant to the biodegradation process, creating toxic compounds in the environment that will eventually enter the food chain (Aragay et al., 2012). The properties of graphene-based porous materials make them promising for pesticide sensing and removal from aqueous environments (Aragay et al., 2012; Maliyekkal et al., 2013), especially the many possibilities for decoration and functionalization. The studies in this direction are promising and are summarized in Table 1.

It is essential to point out that for this and other tables, individual readings of the original articles were performed to obtain the values of the evaluated parameters. Thus, when we represent the value by "NI," we indicate that the value for that parameter is not informed in the original text. This lack of information was observed for all classes of contaminants evaluated in this work, where important information, such as contact time, adsorbent dosage, initial analyte concentration, and evaluated pH range, are not presented. Still, despite not being mandatory, the value of the specific surface area is desirable, and in many works, it was also not present.

Few studies have investigated the ability to remove pesticides from water using three-dimensional graphene materials, especially when considering the environmental importance of these contaminants. Furthermore, most studies do not evaluate the same analyte; the commonly tested are atrazine, glyphosate, and hexaconazole (Andrade et al., 2019; Li et al., 2019; Nodeh et al., 2019; Wang et al., 2019b; Zhang et al., 2015a). There are two studies for each; for the other analytes investigated, only one material was tested for each pesticide. Thus, it becomes challenging to make a comparison between analytes and materials. With the reports available in the literature

Table 1 Adsorption efficiency of materials based on three-dimensional graphene in the adsorption of pesticides

Adsorbate	Adsorbent	Contact time (h)	Adsorbent dose (g/L)	Evaluated pH range	Initial concentration (mg/L)	Specific surface area (m^2/g)	Adsorptive capacity*	Reference
Ametryn	Cellulose/graphene composite[b]	NI	3	9	0.3–15	NI	~95% (0.31 mg/g)	Zhang et al., (2015a)
Atrazine	Graphene oxide impregnated with iron oxide nanoparticles[a]	24	1	12	500–4000	17.68	42.5 mg/g	Andrade et al. (2019)
	Cellulose/graphene composite[b]	NI	3	9	0.3–15	NI	~97% (0.32 mg/g)	Zhang et al., (2015a)
Chlorpyrifos	Glucamine-calix[4]arene functionalized magnetic graphene oxide[a]	2	1	3–10	5–100	NI	78.74 mg/g	Nodeh et al (2019)
Cyprazine	Cellulose/graphene composite[b]	NI	3	9	0.3–15	NI	~91% (0.30 mg/g)	Zhang et al., (2015a)
Epoxiconazole	Graphene/Fe_3O_4 nanocomposite[b]	0.33	0.66	2–13	0–180	NI	~88% (44 mg/g)	Wang et al., (2019b)
Flutriafol	Graphene/Fe_3O_4 nanocomposite[b]	0.33	0.66	2–13	0–180	NI	~92% (46 mg/g)	Wang et al., (2019b)
Glyphosate	Graphene oxide impregnated with iron oxide nanoparticles[a]	24	1	2–12	1–80	19.33	46.8 mg/g	Santos et al. (2019)
	Carboxylated carbon nanotubes-graphene oxide aerogels[a]	NI	NI	NI	NI	NI	546 mg/g	Liu et al., (2019a, b)
Hexaconazole	Graphene/Fe_3O_4 nanocomposite[b]	0.33	0.66	2–13	0–180	NI	~93% (46.5 mg/g)	Wang et al., (2019b)
	Glucamine-calix[4]arene functionalized magnetic graphene oxide[a]	2	1	3–10	5–100	NI	93.46 mg/g	Nodeh et al. (2019)
Metconazole	Graphene/Fe_3O_4 nanocomposite[b]	0.33	0.66	2–13	0–180	NI	~86% (43 mg/g)	Wang et al., (2019b)
Myclobutanil	Graphene/Fe_3O_4 nanocomposite[b]	0.33	0.66	2–13	0–180	NI	~94% (47 mg/g)	Wang et al., (2019b)
Paclobutrazol	Graphene/Fe_3O_4 nanocomposite[b]	0.33	0.66	2–13	0–180	NI	~87% (43.5 mg/g)	Wang et al., (2019b)
Paraquat	3D graphene	24	0.19	6	5–400	103.5	119 mg/g	Huang et al. (2014)
Penconazole	Graphene/Fe_3O_4 nanocomposite[b]	NI	NI	2–13	0–180	NI	~92% (46 mg/g)	Wang et al., (2019b)
Prometryn	Cellulose/graphene composite[b]	NI	3	9	0.3–15	NI	~72% (0.24 mg/g)	Zhang et al., (2015a)

Table 1 (continued)

Adsorbate	Adsorbent	Contact time (h)	Adsorbent dose (g/L)	Evaluated pH range	Initial concentration (mg/L)	Specific surface area (m^2/g)	Adsorptive capacity*	Reference
Simazine	Cellulose/graphene composite[b]	NI	3	9	0.3–15	NI	~85% (0.28 mg/g)	Zhang et al., (2015a)
Simeton	Cellulose/graphene composite[b]	NI	3	9	0.3–15	NI	~88% (0.29 mg/g)	Zhang et al., (2015a)
Tebuconazole	Graphene/Fe_3O_4 nanocomposite[b]	0.33	0.66	2–13	0–180	NI	~97% (48.5 mg/g)	Wang et al., (2019b)
Triadimenol	Graphene/Fe_3O_4 nanocomposite[b]	0.33	0.66	2–13	0–180	NI	~90% (45 mg/g)	Wang et al., (2019b)
Triazolone	Graphene/Fe_3O_4nanocomposite[b]	0.33	0.66	2–13	0–180	NI	~86% (43 mg/g)	Wang et al., (2019b)

NI not informed in the original paper

[a]Functionalized nanomaterial

[b]Composite nanomaterial

*The authors of this article calculated the removal efficiency values in mg/g, presented in parentheses, for a better comparison between the results

that large surface areas provide great adsorptive capabilities, it would be of great interest to compare these data. However, for the works carried out with pesticides, only three studies present the surface areas of the materials used (Andrade et al., 2019; Huang et al., 2014; Santos et al., 2019). This unavailability of data makes it impossible to compare this information with other analytes, as will be shown later.

For the studies in the literature, three-dimensional materials are composed only of graphene (Huang et al., 2014), decorated with iron (Andrade et al., 2019; Mahpishanian & Sereshti, 2016; Santos et al., 2019; Wang et al., 2019a, b), cellulose (Zhang et al., 2015a), glucamine-calix[4]arene (Nodeh et al., 2019), and carbon nanotubes (Liu et al., 2019a) were employed. The works reported that the graphene oxide impregnated with iron oxide nanoparticles showed an adsorption capacity of 42.5 mg/g (Andrade et al., 2019), and a 3D graphene/Fe_3O_4 nanocomposite showed an adsorption capacity of up to 48.5 mg/g (Wang et al., 2019b). Despite the rough comparison between different analytes, due to the lack of analytical repetition of the studies, we noticed that the presence of iron in the samples results in similar adsorption capacities, despite the significant difference in time in which the materials were left for adsorption (about 72 times). This brief observation allows us to infer that more parameters are related to the adsorption of materials than just their composition. The material formed only by 3D graphene showed an adsorptive capacity of 119 mg/g for paraquat. The one that presented the best performance was the graphene-carbon oxide nanotube aerogel, which removed 546 mg/g of glyphosate. Despite the good performances, these materials were tested only for these pesticides, making any comparison unfeasible.

In this sense, we emphasize the importance of conducting more in-depth studies on the influence of the functionalization of three-dimensional graphene materials and the need to present more complete data in published articles. It is imperative that data from adsorption studies, such as adsorbent dosage and contact time, be shown very clearly. In many studies, it was observed that the experimental adsorption procedures are presented in a much-summarized way, limiting the possibilities of comparisons between the studies.

4 Drugs

Drugs are a large group of chemicals employed mainly for medical and health purposes. However,

extensive use has led to higher concentrations of the drugs found in aqueous environments. These chemicals are released into water bodies by the sewers, carrying residues from drug industries, hospitals, and houses (Mackul'ak et al., 2015; Oğuz & Mihçiokur, 2014). This affects the water supplies, which have traces of several drugs—the most common are antibiotics, painkillers, and hormones. Furthermore, these drugs affect the environment, leading to substantial health issues such as the emergence of multidrug-resistant bacteria (Jones et al., 2017). This way, these molecules must be removed from the water before reaching the water environment. However, there is a high cost in the current technologies for drug removal from water (Farzin et al., 2020). Consequently, new methods based on 3D graphene/GO materials, shown in Table 2, have emerged as promising new technologies to remove drugs from water.

The drug class stands out for the low number of published studies. Only studies with antibiotics (ciprofloxacin, norfloxacin, and tetracycline) and anti-inflammatory drugs (diclofenac, ibuprofen, ketoprofen, and naproxen) were found. Few studies report the specific surface area of the materials used and present values that vary between 0.026 (Lu et al., 2020) and 231.38 m^2/g (Ma et al., 2015). For these materials, 3D-rGO with caffeic acid and porous graphene hydrogel, similar adsorption values were found for the two drugs. While the material with a specific surface area of 0.026 m^2/g could adsorb 220.99 mg/g of norfloxacin (Lu et al., 2020), the material with a surface area of 231.38 m^2/g removed 235.6 mg/g of ciprofloxacin (Ma et al., 2015). Despite being different drugs—the comparison between drugs is unfeasible due to the almost inexistence of studies—we observed, once again, that a high specific surface area is not directly related to a high adsorptive capacity.

Analyzing the composition of the materials, we observed that the highest adsorption capacities were found for the hybrid hydrogel 3D reduced graphene oxide/nano Fe_3O_4, capable of removing up to 920 mg/g of ciprofloxacin and 2113 mg/g of tetracycline (Shan et al., 2018). However, as only one material that uses iron in its composition was studied, it is impossible to infer the importance of the presence of iron for these results. In this context, we emphasize the importance of carrying out more studies to evaluate the ability of three-dimensional graphene materials to remove different classes of drugs. So far, studies performed have shown good adsorption capabilities for all material/analyte combinations, indicating that three-dimensional graphene-based materials can remove drugs quite efficiently from water.

5 Other Emerging Contaminants

5.1 Endocrine-Disrupting Chemicals

In addition to the contaminants already described, other classes of contaminants are less studied when referring to their removal through graphene-based three-dimensional nanomaterials. Despite this, they are compounds of great environmental relevance and should be more widely studied. A class that is little studied considering its relevance in the environment is the endocrine interferers. These compounds can interfere in the endocrine system and block or imitate the natural hormones responsible for the functioning of some human or animal body organs. They are commonly detected in wastewater and include bisphenol A, polychlorinated biphenyls, phthalates, polycyclic aromatic hydrocarbons, dichlorodiphenyltrichloroethane, and some heavy metals (Vieira et al., 2020; Zhang et al., 2019). These compounds are proven to cause several adverse effects on human health, which can cause obesity (Darbre, 2017), diabetes (Rancière et al., 2019) and reproductive problems (Cargnelutti et al., 2020), and the ecosystem, which may interfere with the reproductive system of fish, for example (Dang & Kienzler, 2019). Some works have investigated the efficiency of 3D graphene materials, decorated or not, in removing these endocrine-disrupting compounds. The works in this direction are promising and are shown in Table 3.

So far, studies have been published that report the use of pure 3D graphene macrostructures (Wang et al., 2019a) and functionalized with AgBr (Chen et al., 2017a), Ag_3PO_4 (Mu et al., 2017), TiO_2 (Zhang et al., 2018a, b), β-cyclodextrin (Sun et al., 2019), pentaerythritol (Liao et al., 2020), magnesium ascorbyl phosphate (Fang et al., 2018), and mesoporous silica (Wang et al., 2015). A greater number of studies with endocrine disruptors can be found in the literature, but the amount is still low, considering the environmental importance of these compounds. These works allow a more significant discussion of the data, presenting more complete

Table 2 Adsorption efficiency of materials based on three-dimensional graphene in the adsorption of drugs

Adsorbate	Adsorbent	Contact time (h)	Adsorbent dose (g/L)	Evaluated pH range	Initial concentration (mg/L)	Specific surface area (m^2/g)	Adsorptive capacity*	Reference
Ciprofloxacin	Porous graphene hydrogel	2	NI	2–12	0–85	231.38	235.6 mg/g	Ma et al. (2015)
	3D reduced graphene oxide/nano-Fe_3O_4 hybrid hydrogel[b]	NI	0.33	2–8	100–1000	66.8	2.78 mol/g (920 mg/g)	Shan et al. (2018)
	Three-dimensional porous graphene oxide-kaolinite-poly(vinyl alcohol) composite[b]	NI	NI	NI	10–80	NI	408.16 mg/g	Huang et al. (2020)
Diclofenac	Three-dimensional reduced graphene oxide-based hydrogel	NI	NI	4–10	0–296	NI	526.0 mg/g	Umbreen et al. (2018)
Ibuprofen	Three-dimensional reduced graphene oxide-based hydrogel	NI	NI	4–10	0–206	NI	500.0 mg/g	Umbreen et al. (2018)
Ketoprofen	3D-GO with caffeic acid[a]	24	0.2	3–10	10–80	0.026	125.37 mg/g	Lu et al. (2020)
Naproxen	Three-dimensional reduced graphene oxide-based hydrogel	NI	NI	4–10	0–230	NI	357 mg/g	Umbreen et al. (2018)
Norfloxacin	3D GO with caffeic acid[a]	24	0.2	3–10	10–80	0.026	220.99 mg/g	Lu et al. (2020)
Tetracycline	3D reduced graphene oxide/nano-Fe_3O_4 hybrid hydrogel[a]	NI	0.33	2–8	100–1000	66.8	4,76 mmol/g (2113 mg/g)	Shan et al. (2018)
	Soy-graphene aerogel[a]	24	0.5	2–12	0–28	NI	164.0 mg/g	Zhuang et al. (2016)
	Graphene aerogel	24	0.5	2–12	0–28	NI	137.0 mg/g	Zhuang et al. (2016)

NI not informed in the original paper

[a]Functionalized nanomaterial

[b]Composite nanomaterial

*The authors of this article calculated the removal efficiency values in mg/g, presented in parentheses, to compare the results better

Table 3 Adsorption efficiency of materials based on three-dimensional graphene in the adsorption of endocrine disruptors

Adsorbate	Adsorbent	Contact time (h)	Adsorbent dose (g/L)	Evaluated pH range	Initial concentration (mg/L)	Specific surface area (m^2/g)	Adsorptive capacity	Reference
2-Chlorophenol	Three-dimensional foam-like graphene oxide	NI	NI	2–11	0–140	974.8	191.3 mg/g	Wang et al., (2019a)
2,4,6-Trichlorophenol	Three-dimensional foam-like graphene oxide	NI	NI	2–11	0–90	974.8	585.8 mg/g	Wang et al., (2019a)
2,4-Dichlorophenol	Three-dimensional foam-like graphene oxide	NI	NI	2–11	0–120	974.8	398.6 mg/g	Wang et al., (2019a)
3-Nitrophenol	Three-dimensional graphene oxide-pentaerythritol composites[b]	NI	0.25	2–6.5	10–80	1.50	61.1 mg/g	Liao et al. (2020)
4-Chlorophenol	Three-dimensional foam-like graphene oxide	NI	NI	2–11	0–130	974.8	476.2 mg/g	Wang et al., (2019a)
Bisphenol A	Three-dimensional graphene hydrogel-AgBr@rGO[b]	0.5	2	NI	NI	180–220	80.1 mg/g	Chen et al., (2017a)
	Magnesium ascorbyl phosphate graphene-based monolith[a]	48	0.1	2–11	0–130	294.3	324 mg/g	Fang et al. (2018)
	Reduced graphene oxide-β-cyclodextrin aerogel[a]	5	0.1	1–13	0–575	172	346 mg/g	Sun et al. (2019)
	Three-dimensional foam-like graphene oxide	24	0.12	2–11	0–90	974.8	420.9 mg/g	Wang et al., (2019a)
	Ag_3PO_4-graphene hydrogel[a]	0.13	0.5	NI	NI	325.3	15 mg/g	Mu et al. (2017)
	TiO_2-graphene hydrogel with 3D network structure	NI	NI	NI	NI	NI	476.2 mg/g	Zhang et al., (2018a)

Table 3 (continued)

Adsorbate	Adsorbent	Contact time (h)	Adsorbent dose (g/L)	Evaluated pH range	Initial concentration (mg/L)	Specific surface area (m^2/g)	Adsorptive capacity	Reference
Catechol	Three-dimensional graphene aerogels–mesoporous silica frameworks[b]	2	2	NI	87–97	1000.80	66 mg/g	Wang et al. (2015)
Hydroquinone	Three-dimensional graphene aerogels–mesoporous silica frameworks[b]	2	2	NI	83–95	1000.80	67 mg/g	Wang et al. (2015)
	Three-dimensional graphene oxide-pentaerythritol composites[b]	NI	NI	2–6.5	10–80	1.50	42.35 mg/g	Liao et al. (2020)
Phenol	Three-dimensional foam-like graphene oxide	NI	NI	2–11	0–160	974.8	135.6 mg/g	Wang et al., (2019a)
	Three-dimensional graphene aerogels–mesoporous silica frameworks[b]	2	2	NI	85–99	1000.80	90 mg/g	Wang et al. (2015)
Resorcinol	Three-dimensional graphene aerogels–mesoporous silica frameworks[b]	2	2	NI	NI	1000.80	22 mg/g	Wang et al. (2015)
Tert-butylphenol	Three-dimensional graphene oxide-pentaerythritol composites[b]	NI	0.25	2–6.5	10–80	1.50	29.76 mg/g	Liao et al. (2020)

NI not informed in the original paper

[a]Functionalized nanomaterial

[b]Composite nanomaterial

data, such as the surface area for most evaluated materials. Many factors are involved in the contaminant's adsorption efficiency in 3D-based graphene materials. In Fig. 2, we present a graph constructed to relate the adsorptive contaminant capacities of the materials with their specific surface area.

The purpose of constructing these graphs was to compare the relationship between the adsorption

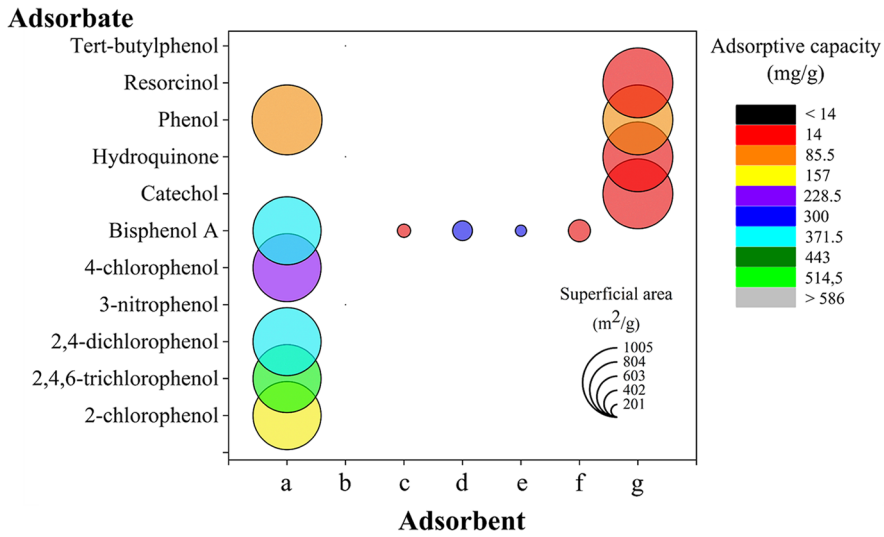

Fig. 2 Specific surface area versus adsorption capacity for each material as a function of the analyte investigated endocrine disruptors. The scale factor is 0.1. *X*-axis caption: **a** Wang et al., (2019a, b); **b** Liao et al. (2020); **c** Chen et al., (2017a); **d** Fang et al. (2018); **e** Sun et al. (2019); **f** Mu et al. (2017); and **g** Wang et al. (2015)

efficiency and the surface area of the materials. If a positive correlation was observed, the larger the bubble, the greater the tendency for the color to be greenish. On the other hand, the smaller the bubble, the greater the tendency for the color to be reddish. A result like this would indicate that the greater the surface area (ie, the bubble), the greater the adsorptive capacity, and vice versa.

It is important to note that this and similar graphs follow different scaling factors for better data visualization, as the figure legend explains. These graphs make it possible to evaluate the effects of the surface area (m^2/g) on the pollutant's adsorption. Unfortunately, it was impossible to make the same comparisons for drugs and pesticides due to the low availability of data, especially for specific surface areas.

In general, many studies claim that good adsorption is directly related to the high surface area of the material; however, analyzing the data, we see that such a correlation is not observed. In Fig. 2, which presents data on endocrine disruptors, materials *a* (three-dimensional foam-like graphene oxide) (Wang et al., 2019a) and *g* (three-dimensional graphene aerogels–mesoporous silica frameworks) (Wang et al., 2015) have similar surface areas. However, different degrees of removal are observed between the materials, and for the same material *a*, we also observe different degrees of removal according to the analyzed analyte (135.6–585.8 mg/g) (Wang et al., 2019a). Most of the materials had similar areas for bisphenol-A, and the adsorption results had relatively slight variation, except for material *a*, which did not show prominent adsorption, despite its high surface area. This is probably due to the composition of the material used, a three-dimensional foam-like graphene oxide, which has a hydrophobic character. We also observed that the lowest bisphenol A removal values were found in materials functionalized with Ag, suggesting that this analyte-adsorbent interaction is inefficient.

5.2 Hydrocarbons

Hydrocarbons (HCs) can reach the environment through oil spills, fossil fuels, and organic pollutants. In addition, these compounds can cause diverse effects on biota and ecosystems, decreasing chlorophyll levels and altering leaf structures in tropical forests, and reducing microbiota diversity (Agathokleous et al., 2020). Recently, the removal of hydrocarbons has also become the goal of developing many three-dimensional materials based on graphene. All these results are summarized in Table 4. In this table, we also present the contact angle values of the materials. This characterization is used to assess the wettability of a surface (Erbil, 2021; Huhtamäki et al., 2018; Song & Fan, 2021), and its value is a measure of the probability that the surface is wetted by water. The smaller the value of the contact angle, the greater the tendency of the water to spread and adhere to the surface. High contact angle values, on the other hand, show

Table 4 Adsorption efficiency of materials based on three-dimensional graphene in the adsorption of hydrocarbons

Adsorbate	Adsorbent	Contact time (min)	Contact angle (°)	Specific surface area (m^2/g)	Removal efficiency*	Reference
Acetone	Three-dimensionally macroporous graphene oxides	NI	107.86	108.97	~180 g/g	Park and Kang (2016)
	Three dimensional graphene/polyurushiol composite[b]	5	136	402.90	38.5 g/g	Zheng et al. (2018)
	Three-dimensional nitrogen and boron codoped graphene[a]	NI	NI	169.9	~1675% (16.75 g/g)	Liu et al., (2017c)
	Three-dimensional superhydrophobic porous hybrid monoliths	NI	156	153.9	~4400% (44.0 g/g)	Chen et al., (2014a)
	Aerogel based on an interpenetrating network of konjac glucomannan and reduced graphene oxide[a]	5	150.3	NI	66 g/g	Luo et al. (2020)
	Hyperelastic and ultra-light magnetic reduced graphene oxide (rGO-Fe_3O_4) 3D framework[a]	5	NI	NI	149.1 g/g	Wang et al., (2020c)
CCl_4	Three dimensional graphene/polyurushiol composite[b]	5	136	402.90	88.8 g/g	Zheng et al. (2018)
$CHCl_3$	Three dimensional graphene/polyurushiol composite[b]	5	136	402.90	83.1 g/g	Zheng et al. (2018)
Chlorobenzene	Three-dimensionally macroporous graphene oxides	NI	107.86	108.97	~240 g/g	Park and Kang (2016)
Chloroform	Three-dimensionally macroporous graphene oxides	NI	107.86	108.97	~310 g/g	Park and Kang (2016)
	Three-dimensional nitrogen and boron codoped graphene[a]	NI	NI	169.9	~1800% (18.0 g/g)	Liu et al., (2017a, b, c)
Corn germ oil	Carbon aerogels based on cellulose nanofibers/poly (vinyl alcohol)/graphene oxide[a]	10	156	NI	~58 g/g	Xu et al., (2018b)
Crude oil	Three-dimensional graphene sponges	NI	NI	NI	~35 g/g	Bagoole et al. (2018)
Cyclohexane	Three-dimensional nitrogen and boron codoped graphene[a]	NI	NI	169.9	~1750% (17.5 g/g)	Liu et al., (2017a, b, c)
	Aerogel based on an interpenetrating network of konjac glucomannan and reduced graphene oxide[a]	5	150.3	NI	54 g/g	Luo et al. (2020)
	Hyperelastic and ultra-light magnetic reduced graphene oxide (rGO-Fe_3O_4) 3D framework[a]	5	NI	NI	239.7 g/g	Wang et al., (2020a, b, c)

Table 4 (continued)

Adsorbate	Adsorbent	Contact time (min)	Contact angle (°)	Specific surface area (m^2/g)	Removal efficiency*	Reference
Dichloromethane	Aerogel based on an interpenetrating network of konjac glucomannan and reduced graphene oxide[a]	5	150.3	NI	82 g/g	Luo et al. (2020)
	Hyperelastic and ultra-light magnetic reduced graphene oxide (rGO-Fe_3O_4) 3D framework[a]	5	NI	NI	308 g/g	Wang et al., (2020a, b, c)
Diesel oil	Aerogel based on an interpenetrating network of konjac glucomannan and reduced graphene oxide[a]	5	150.3	NI	66 g/g	Luo et al. (2020)
	Three-dimensionally macroporous graphene oxides	NI	107.86	108.97	~200 g/g	Park and Kang (2016)
	Three-dimensional chitosan–graphene oxide aerogel[a]	NI	NI	641.6	12.56 g/g	Guo et al. (2016)
	Three-dimensional graphene sponges	NI	NI	NI	~86 g/g	Bagoole et al. (2018)
DMF	Three-dimensional graphene/polyurushiol composite**	5	136	402.90	70.3 g/g	Zheng et al. (2018)
	Carbon aerogels based on cellulose nanofibers/poly (vinyl alcohol)/graphene oxide[a]	10	156	NI	~57 g/g	Xu et al., (2018a, b)
Dodecane	Three-dimensional nitrogen and boron codoped graphene[a]	NI	NI	169.9	~1500% (15.0 g/g)	Liu et al., (2017a, b, c)
	Three-dimensional superhydrophobic porous hybrid monoliths	NI	156	153.9	~3650% (36.5 g/g)	Chen et al., (2014a, b)
Engine oil	Carbon aerogels based on cellulose nanofibers/poly (vinyl alcohol)/graphene oxide[a]	10	156	NI	~72 g/g	Xu et al., (2018a, b)
	Aerogel based on an interpenetrating network of konjac glucomannan and reduced graphene oxide[a]	5	150.3	NI	74 g/g	Luo et al. (2020)

Table 4 (continued)

Adsorbate	Adsorbent	Contact time (min)	Contact angle (°)	Specific surface area (m^2/g)	Removal efficiency*	Reference
Ethanol	Three-dimensionally macroporous graphene oxides	NI	107.86	108.97	~180 g/g	Park and Kang (2016)
	Three-dimensional nitrogen and boron codoped graphene[a]	NI	NI	169.9	~1150% (11.5 g/g)	Liu et al., (2017a, b, c)
	Three-dimensional superhydrophobic porous hybrid monoliths	NI	156	15,309	~4700% (47.0 g/g)	Chen et al., (2014a, b)
	Carbon aerogels based on cellulose nanofibers/poly (vinyl alcohol)/graphene oxide[a]	10	156	NI	~62 g/g	Xu et al., (2018a, b)
	Aerogel based on an interpenetrating network of konjac glucomannan and reduced graphene oxide[a]	5	150.3	NI	60 g/g	Luo et al. (2020)
Ethyl acetate	Three-dimensional superhydrophobic porous hybrid monoliths	NI	156	153.9	~3300% (33.0 g/g)	Chen et al., (2014a, b)
	Hyperelastic and ultra-light magnetic reduced graphene oxide (rGO-Fe_3O_4) 3D framework[a]	5	NI	NI	215.8 g/g	Wang et al., (2020a, b, c)
Gasoline	Carbon aerogels based on cellulose nanofibers/poly (vinyl alcohol)/graphene oxide[a]	10	156	NI	~97 g/g	Xu et al., (2018a, b)
Heptane	Three-dimensional superhydrophobic porous hybrid monoliths	NI	156	153.9	~4000% (40.0 g/g)	Chen et al., (2014a, b)
Hexane	Three-dimensional superhydrophobic porous hybrid monoliths	NI	156	153.9	~3600% (36.0 g/g)	Chen et al., (2014a, b)
	Aerogel based on an interpenetrating network of konjac glucomannan and reduced graphene oxide[a]	5	150.3	NI	55 g/g	Luo et al. (2020)
	Three-dimensional graphene sponges	NI	NI	NI	~24 g/g	Bagoole et al. (2018)
Isopropanol	Three-dimensional nitrogen and boron codoped graphene[a]	NI	NI	169.9	~1250% (12.5 g/g)	Liu et al., (2017a, b, c)
Kerosene	Three-dimensional superhydrophobic porous hybrid monoliths	NI	156	153.9	~4300% (43.0 g/g)	Chen et al., (2014a, b)

Table 4 (continued)

Adsorbate	Adsorbent	Contact time (min)	Contact angle (°)	Specific surface area (m^2/g)	Removal efficiency*	Reference
Lubricating oil	Three-dimensional graphene/polyurushiol composite[b]	5	136	402.90	54.5 g/g	Zheng et al. (2018)
Methanol	Three-dimensional graphene/polyurushiol composite[b]	5	136	402.90	47.0 g/g	Zheng et al. (2018)
	Three-dimensional superhydrophobic porous hybrid monoliths	NI	156	153.9	~5000% (50.0 g/g)	Chen et al., (2014a, b)
Olive oil	Three-dimensional graphene sponges	NI	NI	NI	~12 g/g	Bagoole et al. (2018)
Paraffin oil	Three-dimensional nitrogen and boron codoped graphene[a]	NI	NI	169.9	~2300% (23.0 g/g)	Liu et al., (2017a, b, c)
	Three-dimensional superhydrophobic porous hybrid monoliths	NI	156	153.9	~5000% (50.0 g/g)	Chen et al., (2014a, b)
Petroleum ether	Three-dimensional nitrogen and boron codoped graphene[a]	NI	NI	169	~1000% (10 g/g)	Liu et al., (2017a, b, c)
	Three-dimensional superhydrophobic porous hybrid monoliths	NI	156	153.9	~3500% (35.0 g/g)	Chen et al., (2014a, b)
	Aerogel based on an interpenetrating network of konjac glucomannan and reduced graphene oxide[a]	5	150.3	NI	50 g/g	Luo et al. (2020)
Phenixin	Three-dimensional nitrogen and boron codoped graphene[a]	NI	NI	169.9	~1350% (13.5 g/g)	Liu et al., (2017a, b, c)
Pump oil	Three-dimensionally macroporous graphene oxides	NI	107.86	108.97	~250 g/g	Park and Kang (2016)
	Three-dimensional graphene/polyurushiol composite[b]	5	136	402.90	61.4 g/g	Zheng et al. (2018)
	Three-dimensional nitrogen and boron codoped graphene[a]	NI	NI	169.9	~2050% (20.5 g/g)	Liu et al., (2017a, b, c)
	Three-dimensional superhydrophobic porous hybrid monoliths	NI	156	153.9	~3400% (34.0 g/g)	Chen et al., (2014a, b)
	Carbon aerogels based on cellulose nanofibers/poly (vinyl alcohol)/graphene oxide[a]	10	156	NI	~88 g/g	Xu et al., (2018a, b)
	Aerogel based on an interpenetrating network of konjac glucomannan and reduced graphene oxide[a]	5	150.3	NI	84 g/g	Luo et al. (2020)

Table 4 (continued)

Adsorbate	Adsorbent	Contact time (min)	Contact angle (°)	Specific surface area (m^2/g)	Removal efficiency*	Reference
Q,4-dioxane	Three-dimensional superhydrophobic porous hybrid monoliths	NI	156	153.9	~4450% (44.5 g/g)	Chen et al., (2014a, b)
Rice oil	Three-dimensional nitrogen and boron codoped graphene[a]	NI	NI	169.9	~2200% (22.0 g/g)	Liu et al., (2017a, b, c)
Sesame oil	Hyperelastic and ultra-light magnetic reduced graphene oxide (rGO-Fe_3O_4) 3D framework[a]	5	NI	NI	204.7 g/g	Wang et al., (2020a, b, c)
Soybean oil	Three-dimensional graphene/polyurushiol composite[b]	5	136	402.90	55.5 g/g	Zheng et al. (2018)
	Carbon aerogels based on cellulose nanofibers/poly (vinyl alcohol)/graphene oxide[a]	10	156	NI	~75 g/g	Xu et al., (2018a, b)
	Aerogel based on an interpenetrating network of konjac glucomannan and reduced graphene oxide[a]	5	150.3	NI	72 g/g	Luo et al. (2020)
Tetrachloromethane	Aerogel based on an interpenetrating network of konjac glucomannan and reduced graphene oxide[a]	5	150.3	NI	92 g/g	Luo et al. (2020)
THF	Three dimensional graphene/polyurushiol composite[b]	5	136	402.90	51.0 g/g	Zheng et al. (2018)
Toluene	Three-dimensionally macroporous graphene oxides	NI	107.86	108.97	~200 g/g	Park and Kang (2016)
	Three-dimensional nitrogen and boron codoped graphene[a]	NI	NI	169.9	~2250% (22.5 g/g)	Liu et al., (2017a, b, c)
	Aerogel based on an interpenetrating network of konjac glucomannan and reduced graphene oxide[a]	5	NI	NI	64 g/g	Luo et al. (2020)
Used pump oil	Carbon aerogels based on cellulose nanofibers/poly (vinyl alcohol)/graphene oxide[a]	10	156	NI	~65 g/g	Xu et al., (2018a, b)

NI not informed in the original paper

[a]Functionalized nanomaterial

[b]Composite nanomaterial

*The authors of this article calculated the removal efficiency values in g/g, presented in parentheses, to compare the results better

a tendency of the surface to repel water (Huhtamäki et al., 2018). This characterization can be used to understand chemical structures or physical properties of solid surfaces and their influence on physical

and chemical processes, such as adsorption (Song & Fan, 2021).

Despite the large volume of combinations, only nine studies were carried out in this regard. In addition to materials that use only graphene structures (Bagoole et al., 2018; Chen et al., 2014b; Park & Kang, 2016), functionalized materials with polyurushiol (Zheng et al., 2018), nitrogen and boron codoped (Liu et al., 2017a, b, c), kononic glucomannan (Luo et al., 2020), Fe_3O_4 (Wang et al., 2020a, b, c), chitosan (Guo et al., 2016), and cellulose/poly(vinyl alcohol) (Xu et al., 2018a, b) were used. Overall, the materials removed large amounts of hydrocarbons, mainly the three-dimensional macroporous graphene oxides, which could remove up to 310 times their mass (Park & Kang, 2016). Even the least efficient materials removed at least 11 times their mass (Guo et al., 2016; Liu et al., 2017a, b, c). These results indicate that even the least efficient materials are auspicious for removing hydrocarbons from aquatic environments.

In Fig. 3a, where the results of the hydrocarbons are shown, we observe a similar behavior to the previous one since the material *a* (three-dimensionally macroporous graphene oxide) (Park & Kang, 2016), with the highest adsorptive capacity (310 g/g), is also the one with the smallest area surface of the materials studied for this class of pollutants (108.97 m^2/g). At the same time, the materials with the largest surface areas are those with the lowest removal efficiency. These results show that there is no correlation between specific surface area and hydrocarbon removal efficiency using graphene-based three-dimensional nanomaterials. In this case, using non-functionalized materials seems to have been more efficient, probably due to hydrophobic or pi–pi interactions.

Another graph was also built to evaluate the hydrocarbon removal efficiency as a function of the contact angle (Fig. 3b), which allows us to evaluate the wetting of the adsorbent by the adsorbate. In this, it is possible to observe that material *a*, with greater removal efficiency, has the smallest contact angle (107.86°) (Park & Kang, 2016). However, previous studies reveal no clear trend between the ability to remove hydrocarbons and the contact angle (Yousefi et al., 2019).

Studies showing the efficiency of graphene-based three-dimensional nanomaterials in removing emerging contaminants are increasingly frequent. The papers published to date include the most significant environmental contaminants; however, there are still no studies describing the interaction between these materials with cosmetics and cleaning products in general. Thus, there is a need to include these compounds in future studies. There is still a significant gap in experimental and theoretical combination studies explaining the mechanisms that involve selectivity among different pollutants.

On the other hand, the classes of contaminants that are not considered emerging contaminants are heavy metals and dyes; however, due to their environmental importance, we decided to present the adsorption studies for these 3D graphene materials in the following sections.

6 Heavy Metals

Heavy metals are naturally observed in aqueous systems. Atmospheric deposition or precipitation, or the release and transport of heavy metals from sediments, rocks, and soil, are examples of natural phenomena (Bezerra et al., 2014). However, human-made phenomena are enhancing—at an increasing rate—the presence of this kind of pollutant in water environments. Mining and mineral processing (Abouian Jahromi et al., 2020; Liu et al., 2019a, b; Roche et al., 2017) or the excessive use of pesticides (Wang et al., 2020a) are the primary forms of heavy metals insertion in water. The wastewater of mining dams is filled with water mixtures and elevated amounts of heavy metals. The geochemical process in these mining residues and metallurgic sub-products can contaminate the soil, water streams, and groundwater, affecting the entire food chain (Gomes et al., 2019; Hussain et al., 2013; Kumar et al., 2020; Li et al., 2019; Mao et al., 2019). Therefore, removing the heavy metal excess from mining wastewater is essential, even when the water is appropriately dammed (Da'na, 2017).

Nonetheless, there is another critical issue. Industries and governments can and should avoid anthropogenic disasters at all costs (Edwards & Laurance, 2015; Freitas et al., 2019b; Munhoz, 2019; Roche et al., 2017; Santamarina et al., 2019). However, the Samarco and Vale recent dam break in Brazil (Burritt & Christ, 2018; Freitas et al., 2019a; Heller, 2019) are clear examples that negligence can lead to huge

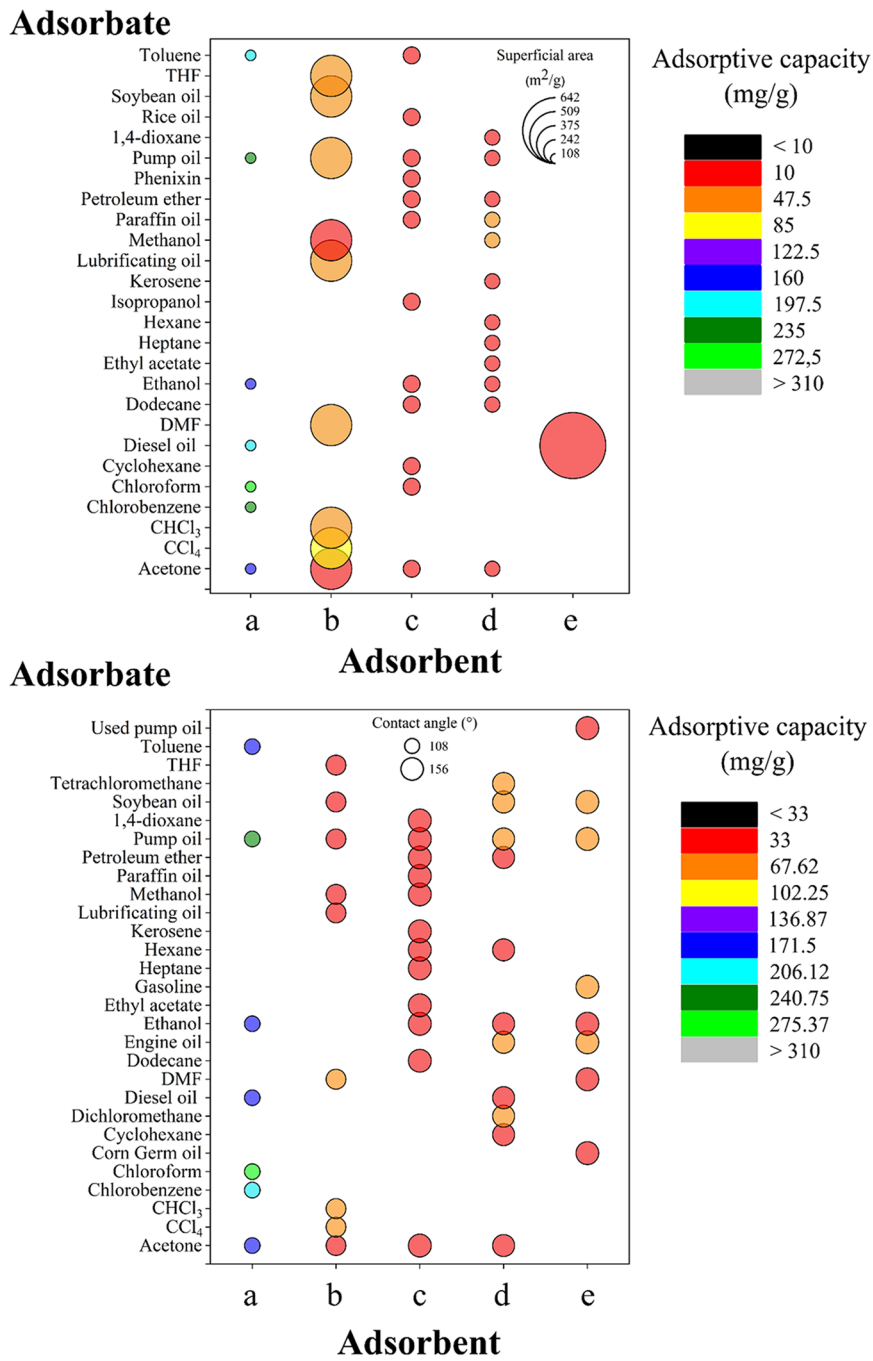

Fig. 3 Specific surface area versus adsorption capacity for each material as a function of the analyte investigated for hydrocarbons (**a**) and contact angle versus adsorption capacity for each material (**b**). The scale factors are, respectively, 0.17 and 0.25. *X*-axis caption: **a** Park & Kang (2016); **b** Zheng et al. (2018); **c** Liu et al., (2017c); **d** Chen et al., (2014b); and **e** Guo et al. (2016)

disasters (Almeida et al., 2019; Garcia et al., 2017; Guardian, 2018; Labonne, 2016; Tuncak., 2017). The consequences led not only to economic and social impacts but to extensive and still not wholly understood environmental (Almeida et al., 2018; Burritt & Christ, 2018; Cordeiro et al., 2019; Gomes et al., 2019; Queiroz et al., 2018) and health (Burritt & Christ, 2018; Carrillo et al., 2019; Freitas et al., 2019b; Noal et al., 2019) impact. In this sense, and considering that the cited Brazilian examples are not isolated cases (Bezerra et al., 2014; Lee et al., 2006; Owen et al., 2020; Rico et al., 2008), the rise of new technologies is urgent to prevent (de Souza, 2019) and remedy these disasters. Recent studies have

shown that graphene-based nanomaterials can be employed for heavy metal adsorption (Bodzek et al., 2020). The negatively charged sites that remain after the chemical graphene oxide reduction facilitate this process once most heavy metals are cationic (Chen et al., 2018). In this section, we discuss the new and promising graphene-based technologies for heavy metal removal from water. The main heavy metal adsorption capacities of 3D materials are summarized in Table 5.

Unlike organic analytes, which have fewer studies, numerous research papers can be found on heavy metals. This allows a better comparison between the efficiency of different materials for the same analyte. Materials that adsorb large or small amounts of metals and small or large specific surface areas can be found for these studies. In Fig. 4, data for heavy metals are shown. It is possible to verify that the *d* material (Li et al., 2013) with high-density three-dimension graphene macroscopic objects presented a specific surface area of 560 m^2/g and elevated copper adsorptive capacity (ca. 3820 mg).

On the other hand, material *r* (Amini et al., 2021) was the material with the most significant specific surface area (1350 m^2/g). However, its adsorptive capacity for uranium was 416.7 mg/g, similar to those obtained by material *a* for other contaminants, which had a specific surface area about 11 times smaller than *r*. Bare, oxidized, carbon-based nanomaterials with varying modifications have been used to adsorb heavy metals from aqueous environments. Although previous reviews show that greater adsorption capacities are achieved after functionalization (Xu et al., 2018a), this behavior was not observed systematically.

We can analyze more specifically and compare different materials used for the same analyte. The metal that presents the most striking result is Uranium. The material *p* (Wang et al., 2017), which does not even appear in Fig. 4 due to its very low surface area, has an adsorptive capacity quite similar to that of material *r* (Amini et al., 2021), which has the largest surface area of all materials studied for metal removal, around 54 thousand times greater than *p*. As for Pb, we observed that material *b* (Chen et al., 2014a, 2b) showed a high adsorptive capacity (399.3 mg/g) despite having a low surface area (0.062 m^2/g). On the other hand, for material *e* (Lei et al., 2014a), we observed a completely different behavior: despite having a significantly larger surface area than material b (578.4 m^2/g); it has a capacity very similar to 381.3 mg/g. In common, none of these materials has been functionalized, indicating that other parameters must explain these values. For copper, three materials have relatively similar surface areas (345–560 m^2/g), but the adsorptive capacities varied between 25.4 and 3820 mg/g. While the highest value was found using non-functionalized high-density three-dimensional graphene macroscopic objects (Li et al., 2013), the lowest value was found in a material functionalized with chitosan (Yu et al., 2013).

7 Dyes

Synthetic organic dyes are essential to fulfill the human demands in quality, variety, celerity, and other technical requirements, for coloring a growing number of materials, from clothes and cars to beverages and food (Tkaczyk et al., 2020) . One of the chemical industry main concerns is that many synthetic dyes are lost in product manufacturing. For instance, 10 to 15% of all dye is carried out to effluent water (Ananthashankar, 2012; Hassaan & Nemr, 2017). This leads to changes in the watercolor and the biological oxygen supply (Wang et al., 2007). Therefore, it is urgent to create new materials to reduce the due pollution of dyes in water. In this way, several researchers have proposed graphene-based structures to remove this pollutant from water. A summary of these studies is shown in Table 6.

Figure 5, we find a behavior similar to those reported in the previous figures. Material *h* (Cheng et al., 2012), which has a higher specific surface area (603.2 m^2/g), presented a low removal efficiency when compared to other studies (7.8 mg/g). Materials *b*, *d*, *f*, *g*, and *k* have the opposite behavior: despite having low surface areas (8.18–154 m^2/g), they showed excellent adsorptive capacities (578–833.3 mg/g) (Chen et al., 2017b; Ma et al., 2014, 2020; Xiao et al., 2018; Zhang et al., 2015a, b). The only material agreeing on the surface area *x* removal efficiency was *j* (476 m^2/g, 800 mg/g) (Sui et al., 2013). About methylene blue, we observed a smaller variation of surface areas in the materials studied; however, the removal values still show a significant variation (90–833.3 mg/g). On the one hand, the material with the lowest removal capacity,

Table 5 Adsorption efficiency of materials based on three-dimensional graphene in the adsorption of heavy metals

Adsorbate	Adsorbent	Contact time (h)	Adsorbent dose (g/L)	Evaluated pH range	Initial concentration (mg/L)	Specific surface area (m^2/g)	Adsorptive capacity*	Reference
Ag(I)	Three-dimensional molybdenum disulfide/graphene hydrogel[a]	8	0.17	5.4	NI	118	99% (5.94 mg/g)	Zhuang et al. (2018)
As(V)	Graphene foam	0.67	0.20	3–10	NI	0.062	177.6 mg/g	Chen et al., (2014b)
Cd(II)	Polydopamine-functionalized graphene hydrogel[a]	12	0.10	2–6	0–500	310.6	145.48 mg/g	Gao et al. (2013)
	High-density three-dimension graphene macroscopic objects	NI	NI	NI	NI	560	434 mg/g	Li et al. (2013)
	Graphene oxide aerogels by layered double hydroxides[a]	1.33	NI	NI	NI	NI	95.67 mg/g	Fang and Chen (2014)
	Three-dimensional graphene oxide foam	NI	0.20	2–10	5–250	578.4	252.5 mg/g	Lei et al., (2014a)
	3D sulfonated reduced graphene oxide[a]	12	0.10	2–9	0–50	330.29	234.8 mg/g	Wu et al. (2015)
	3D graphene/δ-MnO_2 aerogels[a]	24	0.04	2–6	1–200	NI	250.31 mg/g	Liu et al. (2016)
	Phosphorylethanolamine-functionalized super-hydrophilic 3D graphene-based foam[a]	NI	NI	NI	NI	NI	254.9 mg/g	Chen et al. (2018)
	Graphene-based aerogels	NI	0.90	NI	NI	NI	24.7 mg/g	Yu et al. (2019)
	Three-dimensional molybdenum disulfide/graphene hydrogel[a]	8	0.17	2.9	NI	118	75% (4.48 mg/g)	Zhuang et al. (2018)
	3D porous graphene/lignin/sodium alginate composite	1.67	0.25	NI	0–45	131.4	79.88 mg/g	Zhou et al. (2018)
	Multithiol functionalized graphene biosponge[a]	24	1	4–9	10–100	115	102.99 mg/g	Yap et al. (2020)
Co(II)	Three-dimensional molybdenum disulfide/graphene hydrogel[a]	8	0.17	2.2	NI	118	3% (0.138 mg/g)	Zhuang et al. (2018)
Cr(IV)	Three-dimensional magnetic graphene oxide foam/Fe3O4 nanocomposite[b]	0.5	0.50	1–6	10–200	574.2	258.6 mg/g	Lei et al. (2014b)
	Three-dimensional reduced graphene oxide and montmorillonite composite aerogel[b]	NI	NI	2–11	NI	NI	94.87%	Zhang et al., (2018a, b)
	3D lotus biochar/reduced graphene oxide aerogel[a]	12	0.6	2–10	10–200	NI	232,56 mg/g	Wei et al. (2020)
Cs(I)	Prussian blue analogs anchored on 3D reduced graphene oxide aerogel[a]	48	0.15	3–11	1.7–325	76.2	204.9 mg/g	Huo et al. (2021)

Table 5 (continued)

Adsorbate	Adsorbent	Contact time (h)	Adsorbent dose (g/L)	Evaluated pH range	Initial concentration (mg/L)	Specific surface area (m^2/g)	Adsorptive capacity*	Reference
Cu(II)	Graphene oxide–chitosan composite hydrogels[b]	10	0.12	NI	10–120	NI	70 mg/g	Chen et al., (2013a)
	High-density three-dimension graphene macroscopic objects	NI	NI	NI	NI	560	3820 mg/g	Li et al. (2013)
	Graphene oxide–chitosan aerogel[b]	24	0.62	2–7	1.92–32	345	25.4 mg/g	Yu et al. (2013)
	3D graphene/δ-MnO_2 aerogels[a]	24	0.04	2–6	NI	NI	228.46 mg/g	Liu et al. (2016)
	Xanthan gum–graphene oxide hybrid aerogels[a]	12	0.10	NI	NI	NI	53.2 mg/g	Liu et al., (2017b)
	Amino-functionalized carbon nanotube-graphene hybrid aerogels[b]	24	0.5	2–7	50–400	356.1	318.47 mg/g	Zhan et al. (2019)
	Functionalized graphene oxide/carboxymethyl chitosan composite aerogels[b]	24	NI	NI	25–600	NI	170.3 mg/g	Luo et al., (2021a)
	3D graphene/MnO_2 nanocomposites	24	0.2	NI	NI	490	83.5 mg/g	Zhou et al. (2022)
Fe(II)	Graphene-based aerogels	NI	0.90	NI	NI	NI	67.1 mg/g	Yu et al. (2019)
Fe(III)	Three-dimensional graphene oxide foam	NI	0.20	2–10	5–250	578.4	587 mg/g	Lei et al., (2014b)
Hg(II)	Graphene-based composite with unique 3D architecture composed of graphene nanosheets decorated with αFeOOH nanoparticles and porous diatom silica microparticles[a]	1.5	0.04	2–10	25–375	340.8	> 800 mg/g	Kabiri et al. (2016)
	Amphiphilic PA-induced three-dimensional graphene macrostructure	48	NI	2–12	25–500	NI	361.01 mg/g	Tan et al. (2018)
	Three-dimensional molybdenum disulfide/graphene hydrogel[a]	8	0.17	2.1	0–100	118	100% (5.99 mg/g)	Zhuang et al. (2018)
Ni(II)	High-density three-dimension graphene macroscopic objects	NI	NI	NI	NI	560	1683 mg/g	Li et al. (2013)
	Functionalized graphene oxide/carboxymethyl chitosan composite aerogels[a]	24	NI	NI	25–600	NI	186.8 mg/g	Luo et al., (2021a)

Table 5 (continued)

Adsorbate	Adsorbent	Contact time (h)	Adsorbent dose (g/L)	Evaluated pH range	Initial concentration (mg/L)	Specific surface area (m^2/g)	Adsorptive capacity*	Reference
Pb(II)	Graphene oxide–chitosan composite hydrogels[b]	10	0.12	NI	10–120	NI	90 mg/g	Chen et al., (2013a)
	Polydopamine-functionalized graphene hydrogel[a]	12	0.10	2–6	0–800	310.6	336.32 mg/g	Gao et al. (2013)
	High-density three-dimension graphene macroscopic objects	NI	NI	NI	NI	560	882 mg/g	Li et al. (2013)
	Graphene–carbon nanotube aerogel[b]	24	0.20	NI	NI	NI	230–451 mg/g	Zhang et al. (2013)
	Graphene foam	0.66	0.20	3–10	NI	0.062	399.3 mg/g	Chen et al., (2014b)
	Graphene aerogels	24	0.30	NI	NI	350	80 mg/g	Han et al., (2014
	Three-dimensional graphene oxide foam	NI	0.20	2–10	5–250	578.4	381.3 mg/g	Lei et al., (2014a)
	Lignosulfonate-modified graphene hydrogel[a]	12	NI	2–6	0–300	459.3	1210 mg/g	Li et al. (2016)
	3D graphene/δ-MnO_2 aerogels[a]	24	0.04	2–6	1–200	NI	643.62 mg/g	Liu et al. (2016)
	Phosphorylethanolamine-functionalized Super-hydrophilic 3D graphene-based foam[a]	NI	NI	NI	NI	NI	296 mg/g	Chen et al. (2018)
	Graphene monoliths	48	NI	2–7	0–400	28.52	101.1 mg/g	Fang et al. (2017)
	3D porous graphene	1.67	0.25	1–6	NI	314.5	~150 mg/g	Zhou et al. (2017)
	Graphene-based aerogels	NI	0.90	NI	NI	NI	53.7 mg/g	Yu et al. (2019)
	Three-dimensional molybdenum disulfide/graphene hydrogel[a]	8	0.17	3.1	NI	118	64% (3.82 mg/g)	Zhuang et al. (2018)
	3D porous graphene/lignin/sodium alginate composite	1.67	0.25	NI	0–50	131.4	226.24 mg/g	Zhou et al. (2018)
	Amino-functionalized carbon nanotube-graphene hybrid aerogels[a]	24	0.5	2–7	50–400	356.1	350.87 mg/g	Zhan et al. (2019)
	Multithiol functionalized graphene biosponge[a]	24	1	4–9	10–100	115	101.01 mg/g	Yap et al. (2020)
	Functionalized graphene oxide/carboxymethyl chitosan composite aerogels[b]	24	NI	NI	25–600	NI	312.8 mg/g	Luo et al., (2021a)
	3D graphene/MnO2 nanocomposites	24	0.2	NI	NI	490	247.3 mg/g	Zhou et al. (2022)

Table 5 (continued)

Adsorbate	Adsorbent	Contact time (h)	Adsorbent dose (g/L)	Evaluated pH range	Initial concentration (mg/L)	Specific surface area (m^2/g)	Adsorptive capacity*	Reference
Sr(II)	Foamy-like 3-dimensional graphene networks decorated with iron oxide nanoparticles[a]	NI	NI	NI	5–130	295.55	39.68 mg/g	Kasap (2020)
U(VI)	Melamine-modified graphene hydrogels[a]	3	0.50	NI	3–250	0,025	404.85 mg/g	Wang et al. (2017)
	Three-dimensional ultra-light poly(amidoxime)/graphene oxide nanoribbons aerogel[b]	2	0.20	1–10	0.0238–0.238	494.9	2.475 mmol/g (589.1 mg/g)	Wang et al. (2021)
	Graphene oxide/3D mesoporous MOF nanocomposite[b]	0.05	0.20	3–8	0–700	1350	416,7 mg/g	Amini et al. (2021)
UO_2(II)	3D graphene/MnO_2 nanocomposites	24	0.2	NI	NI	490	172.5 mg/g	Zhou et al. (2022)
Zn(II)	Three-dimensional graphene oxide foam	NI	0.20	2–10	5–250	578.4	32.,4 mg/g	Lei et al., (2014a)
	Three-dimensional molybdenum disulfide/graphene hydrogel[a]	8	0.17	2.9	NI	118	24% (1.42 mg/g)	Zhuang et al. (2018)

NI not informed in the original paper

[a]Functionalized nanomaterial

[b]Composite nanomaterial

*The authors of this article calculated the removal efficiency values in mg/g, presented in parentheses, to compare the results better

90 mg/g, with an area of 182.6 m^2/g, is L-cysteine-reduced graphene oxide/polyvinyl alcohol ultralight aerogel (Xiao et al., 2017). On the other hand, three-dimensional networked porous polyvinyl alcohol/sodium alginate/graphene oxide was the material used in the study with one of the largest additive capacities (759.3 mg/g) despite its low surface area (26.08 m^2/g) (Ma et al., 2020). Such results indicate that the adsorption process can have quite variable results despite using materials with similar functionalization and, still, it is not related to a large specific surface area. For this dye, it was not possible to verify the influence of the use of functionalized materials since good and bad results were found for functionalized materials or not.

These works show how it is possible to select specific pollutants, with specific physical–chemical properties, by tuning the nanocompound properties through functionalization. In general, we can observe that, contrary to what the literature says (Luo et al., 2021a; Yousefi et al., 2019), the surface area does not seem to be directly related to the efficiency in removing contaminants using graphene-based three-dimensional materials. For hydrocarbons, we can mention that an important factor is the contact angle since smaller contact angles provide better adsorptive capacities. For the other classes of contaminants, it was impossible to find a property that could be directly related to the results obtained; however, we can infer that the very constitution of materials, especially composites, has greater importance in the adsorption process. At the same time, as exemplified for materials functionalized with iron, it is not possible to say that a specific material will be a suitable adsorbent for an analyte just by checking its composition.

In addition, other essential factors that must be taken into account are the parameters selected for carrying out the adsorption experiments, such as temperature, pH, ionic strength, agitation, analyte concentration, amount of material, and the ratio of material mass/volume of the analyte and adsorption time. Thus, it is evident that although the specific surface

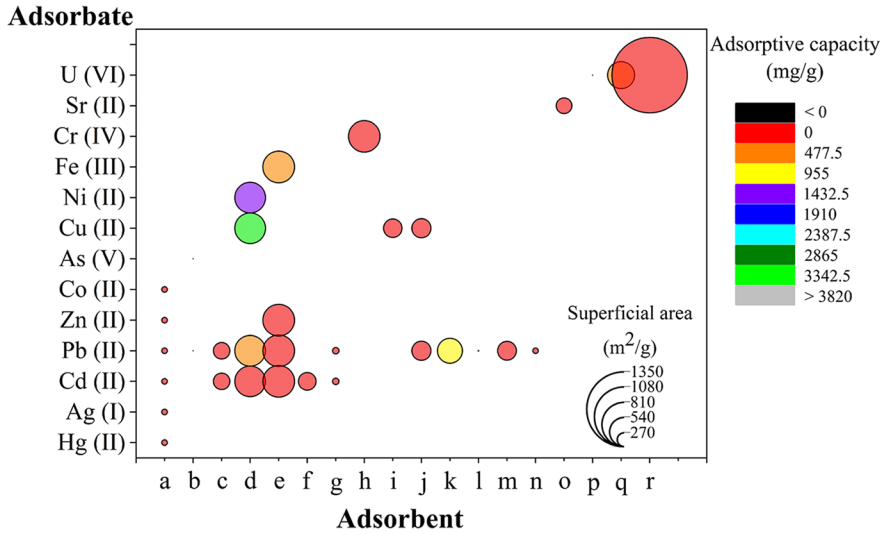

Fig. 4 Specific surface area versus adsorption capacity for each material as a function of the analyte investigated for metals. The scale factor is 0.08. *X*-axis caption: **a** Zhuang et al. (2018); **b** Chen et al., (2014a, b); **c** Gao et al. (2013); **d** Li et al. (2013); **e** Lei et al., (2014a); **f** Wu et al. (2015); **g** Zhou et al. (2018); **h** Lei et al. (2014b); **i** Yu et al. (2013); **j** Zhan et al. (2019); **k** Li et al. (2016); **l** Fang et al. (2017); **m** Han et al. (2014); **n** Yap et al. (2020); **o** Kasap (2020); **p** Wang et al. (2017); **q** Wang et al. (2021); and **r** Amini et al. (2021)

area is a vital factor for adsorption, it should not be concluded that a given material will be a suitable adsorbent just because it has a high specific surface area.

A significant problem observed in the adsorption tests reported in this work is the sizeable experimental variation observed. We found adsorption times that varied between 3 min and 120 h among all the works. Furthermore, the adsorbent dosages (in g of adsorbent per L of adsorbate) varied between 0.03 and 3 g/L. The literature recommends using rates between 0.5 and 3 g/L; however, 67% of the studies used values lower than 0.5 g/L. This condition may overestimate the results obtained since the adsorptive capacity of the materials is given as a function of the adsorbent mass used in the tests. These conditions make it impossible to compare the studies carried out so far. Despite this, there is no doubt that materials based on three-dimensional graphene are up-and-coming for water treatment. A point that should be highlighted is the importance of obtaining 3D structures that are stable when in an aqueous environment. In this review, we observed that most works mention the need for filtration or centrifugation of samples to quantify the analytes after the adsorption procedures. This is due to the dispersion of materials in the solution. Such conditions impair the use of these materials for application in natural systems.

With the construction of the figures, it was possible to observe the number of studies conducted in terms of adsorbates or adsorbents. For metals, it is evident that the most studied are, respectively, Pb(II), Cd(II), and Cu(II). On the other hand, studies with important environmental contaminants, Cr(IV) and Hg(II), are still scarce. There are many studies carried out for dyes with methylene blue, possibly because it is already a dye widely studied for other types of adsorbents; in endocrine disruptors, similar behavior is observed for bisphenol A.

With hydrocarbons, more adsorbents are tested in removing acetone, diesel oil, ethanol, and pump oil. In contrast, for this class, it is observed that the same material was evaluated in the removal of different compounds, while this behavior was observed in only three materials evaluated with metals (*a*, *d,* and *e*), one evaluated with dyes (*a*) and two evaluated with endocrine interferences (a and g).

As a result of the small number of studies carried out with pesticides and drugs, the graphs for these compounds could not be constructed due to insufficient data. It was found that most drugs were studied with only one material, except for ciprofloxacin

Table 6 Adsorption efficiency of materials based on three-dimensional graphene in the adsorption of dyes

Adsorbate	Adsorbent	Contact time (h)	Adsorbent dose (g/L)	Evaluated pH range	Initial concentration (mg/L)	Specific surface area (m^2/g)	Adsorptive capacity*	Reference
Amaranth	Three-dimensional graphene oxide–polyethylenimine[a]	12	0.05	NI	NI	476	800 mg/g	Sui et al. (2013)
	Amino-functionalized ultralight graphene aerogel[a]	12	0.03	2–11	50–300	NI	2043.7 mg/g	Shu et al. (2017)
Cationic dyes	Graphene/nanofiber aerogels[b]	NI	0.25	NI	500	33	> 800 mg/g	Xiao et al. (2018)
Crystal violet	L-Cysteine-reduced graphene oxide/poly(vinyl alcohol) ultralight aerogel[a]	NI	NI	1–7	0–400	182.6	~ 100% (90 mg/g)	Xiao et al. (2017)
Fuchsin	L-Cysteine-reduced graphene oxide/poly(vinyl alcohol) ultralight aerogel[a]	NI	NI	1–7	0–4	182.6	~ 40% (36 mg/g)	Xiao et al. (2017)
	Polyacrylamide/graphene oxide aerogels[b]	70	0.50	2.6–8.9	100–400	NI	1034.3 mg/g	Yang et al. (2015)
Indigo disulfonate	Graphene-based aerogel with rare earth metal oxide	2	0.50	NI	NI	NI	397 mg/g	Pan et al. (2018)
Methyl orange	Three-dimensional (3D) graphene hydrogel	13	0.03	NI	NI	154	70 mg/g	Zhang et al. (2015b)
	Amino-functionalized ultralight graphene aerogel[a]	12	0.03	2–11	NI	NI	3059.2 mg/g	Shu et al. (2017)
	L-Cysteine-reduced graphene oxide/poly(vinyl alcohol) ultralight aerogel[a]	NI	NI	1–7	0–400	182.6	~ 90% (81 mg/g)	Xiao et al. (2017)
	Zeolite imidazolate framework/graphene hybrid aerogels[b]	10	0.20	NI	NI	NI	550.3 mg/g	Hou et al. (2018)
	3D graphene oxide/carbon nanotubes	NI	NI	NI	5–30	257.6	66.96	Hu et al. (2021)

Table 6 (continued)

Adsorbate	Adsorbent	Contact time (h)	Adsorbent dose (g/L)	Evaluated pH range	Initial concentration (mg/L)	Specific surface area (m^2/g)	Adsorptive capacity*	Reference
Methyl violet	Three-dimensional graphene oxide nanostructure	3	2.00	3–10	NI	48.41	467 mg/g	Liu et al. (2012)
	3D graphene oxide gels based	120	0.05	3–11	0–40	NI	1350 mg/g	Deng et al. (2013)
Methylene blue	Three-dimensional graphene oxide nanostructure	3	2.00	3–10	NI	48.41	397 mg/g	Liu et al. (2012)
	3D graphene oxide gels based	70	0.05	3–11	0–40	NI	1100 mg/g	Deng et al. (2013)
	Reduced graphene oxide-based hydrogels	2	0.60	NI	0–0.30	298.2	100%	Tiwari et al. (2013)
	Ultra-light graphene-based gels	24	0.30	NI	0–250	18.98	833.3 mg/g	Ma et al. (2014)
	Three-dimensional (3D) graphene hydrogel	13	0.03	NI	NI	154	660 mg/g	Zhang et al. (2015b)
	Reduced graphene oxide-montmorillonite three-dimensional composite aerogel[b]	1.67	0.20	3–11	5–50	4.163	99.73%	Yan et al. (2016)
	γ-Fe_2O_3 nanocrystals-anchored macro/meso-porous graphene[a]	0.08	0.15	5–11	0–16	154	216.3 mg/g	Zhang et al. (2016)
	Agar/graphene oxide composite aerogel[b]	26	0.40	2–10	0–50	8.18	578 mg/g	Chen et al., (2017b)
	L-cysteine-reduced graphene oxide/poly(vinyl alcohol) ultra-light aerogel[a]	NI	NI	1–7	0–400	182.6	~100% (90 mg/g)	Xiao et al. (2017)
	Three-dimensional (3D) networked porous polyvinyl alcohol/sodium alginate/graphene oxide[a]	8	1.00	1–8	0–2000	26.08	759.3 mg/g	Ma et al. (2020)

Table 6 (continued)

Adsorbate	Adsorbent	Contact time (h)	Adsorbent dose (g/L)	Evaluated pH range	Initial concentration (mg/L)	Specific surface area (m^2/g)	Adsorptive capacity*	Reference
Methylene green	L-cysteine-reduced graphene oxide/poly(vinyl alcohol) ultra-light aerogel[a]	NI	NI	1–7	0–400	182.6	~100% (90 mg/g)	Xiao et al. (2017)
Nonionic red oil dye	L-cysteine-reduced graphene oxide/poly(vinyl alcohol) ultra-light aerogel[a]	NI	NI	1–7	0–400	182.6	~75% (67.5 mg/g)	Xiao et al. (2017)
Orange G	Three-dimensional (3D) graphene hydrogel	13.33	0.03	NI	NI	154	30 mg/g	Zhang et al. (2015b)
Reactive black 5	Three-dimensional chitosan–graphene mesostructures[b]	1.33	0.12	4–8	200–2000	603.2	97.5% (7,8 mg/g)	Cheng et al. (2012)
Rhodamine B	Polydopamine-Functionalized Graphene Hydrogel[a]	12	0.10	2–6	0–600	310.6	207.06 mg/g	Gao et al. (2013)
	Reduced graphene oxide-based hydrogels	2	0.60	NI	0–0.35	298.2	97%	Tiwari et al. (2013)
	Three-dimensional graphene aerogel	10	0.50	NI	25–500	NI	280.8 mg/g	Liu et al., (2017a)
	Zeolite imidazolate framework/graphene hybrid aerogels[b]	12	0.20	NI	NI	NI	380.7 mg/g	Hou et al. (2018)
	3D graphene oxide/carbon nanotubes	NI	NI	NI	10–25	257.6	248.48 mg/g	Hu et al. (2021)

Table 6 (continued)

Adsorbate	Adsorbent	Contact time (h)	Adsorbent dose (g/L)	Evaluated pH range	Initial concentration (mg/L)	Specific surface area (m^2/g)	Adsorptive capacity*	Reference
Safranine	GO/DNA composite hydrogels[b]	12	0.03	2–13	NI	NI	960 mg/g	Xu et al. (2010)
	3D graphene oxide reduced with ascorbic acid 0 mmol/L	6	3.2	NI	0–3500	172.2	381.4 mg/g	Leão et al. (2022)
	3D graphene oxide reduced with ascorbic acid 5 mmol/L	6	3.2	NI	0–3500	163.1	937.8 mg/g	Leão et al. (2022)
	3D graphene oxide reduced with ascorbic acid 10 mmol/L	6	3.2	NI	0–3500	68.9	643.3 mg/g	Leão et al. (2022)
	3D graphene oxide reduced with ascorbic acid 25 mmol/L	6	3.2	NI	0–3500	62.8	247.8 mg/g	Leão et al. (2022)
Starch black	L-Cysteine-reduced graphene oxide/poly(vinyl alcohol) ultra-light aerogel[a]	NI	NI	1–7	0–400	182.6	~100% (90 mg/g)	Xiao et al. (2017)

NI not informed in the original paper

[a]Functionalized nanomaterial

[b]Composite nanomaterial

*The authors of this article calculated the removal efficiency values in mg/g, presented in parentheses, to compare the results better

(Huang et al., 2020; Ma et al., 2015; Shan et al., 2018) and tetracycline (Shan et al., 2018; Zhuang et al., 2016). Despite this, removal efficiencies with significant values were observed. For pesticides, in the same way, repetitions were observed only for glyphosate (Liu et al., 2019a; Santos et al., 2019), atrazine (Andrade et al., 2019; Zhang et al., 2015a), and hexaconazole (Nodeh et al., 2019; Wang et al., 2019a, b). Some materials were developed and tested for different contaminants of the same class, allowing focus on a target analyte in future applications. However, most pesticides have undergone an adsorption process using graphene/iron composite materials (Mahpishanian & Sereshti, 2016; Wang et al., 2019b) and presented low removal values in the mass ratio of adsorbate/mass of adsorbent, resulting in few materials capable of removing large amounts of pesticides.

8 Adsorption Mechanisms

Few studies describe the possible adsorption mechanisms involved in their respective works. The number of articles is even more limited when we look for theoretical–experimental works that could elucidate these mechanisms more clearly. Despite this, it is possible to predict which material-analyte interactions can be found in these studies. Based on Fig. 6, we highlight that the main mechanisms are π–π interactions, pore filling, hydrophobic interactions,

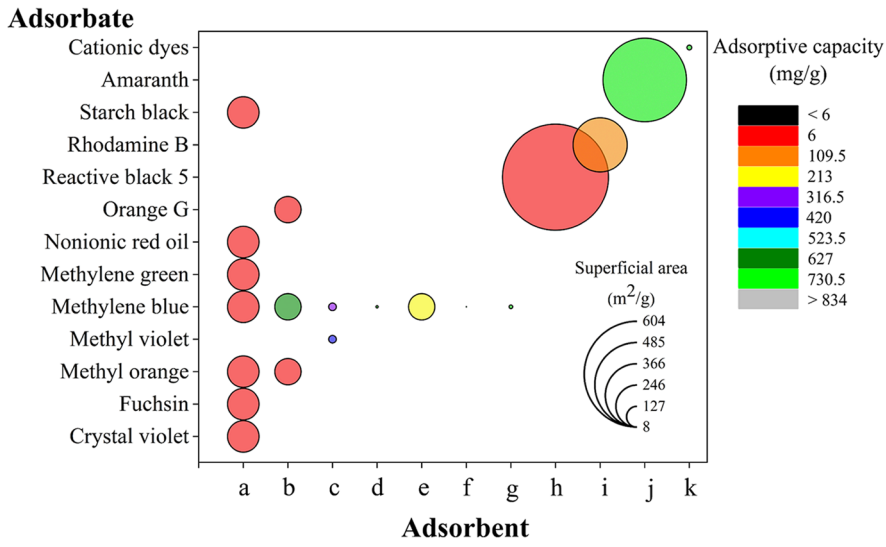

Fig. 5 Specific surface area versus adsorption capacity for each material as a function of the analyte investigated for dyes. The scale factor is 0.25. *X*-axis caption: **a** Xiao et al. (2017); **b** Zhang et al., (2015a, b); **c** Liu et al. (2012); **d** Ma et al. (2014); **e** Zhang et al. (2016); **f** Chen et al., (2017b); **g** Ma et al. (2020); **h** Cheng et al. (2012); **i** Gao et al. (2013); **j** Sui et al. (2013); and **k** Xiao et al. (2018)

electrostatic interactions of attraction or repulsion, and hydrogen bonds, among others.

Structural characteristics, such as the presence of pores, including the type, size, and pores volume, determine the access and entrapment of pollutants within the pores of the adsorbents. Filling pore is primarily responsible for the adsorption of organic pollutants, such as oils and organic solvents. In addition, the chemical structure of the materials is fundamental, which will influence intermolecular interaction. For example, the π–π interaction involves non-covalent attraction between aromatic rings of organic pollutants and graphene sorbents. Hydrogen bonds are a dipole–dipole interaction between a hydrogen atom covalently bonded to highly electronegative atoms such as nitrogen, fluorine, and oxygen in graphene sorbents functionalized with another electronegative atom carrying a lone pair. This attractive force is portrayed when the functional groups grafted onto the sp^3 domains of graphene interact with polar organic contaminants or vice versa. In addition, the hydrophobic interaction occurs between nonpolar organic molecules, such as oils and nonpolar solvents, with the hydrophobic binding sites of graphene sorbents. Finally, electrostatic interactions can significantly contribute to the adsorption of positively or negatively charged pollutants, including cationic heavy metal ions and ionic organic dyes at the binding sites of graphene sorbents (Yap et al., 2021).

Understanding the interaction mechanism between the contaminants and the material used for their adsorption is essential; however, we emphasize that this type of discussion is absent in most of the articles cited in this work. For this reason, our work cannot wholly explore the adsorption mechanisms that may be involved and go beyond the surface area × adsorptive capacity relationship. Instead, based on an individual search in the cited articles, we present a brief discussion based on the interaction mechanisms mentioned above.

For organic compounds, it is common to mention the same mechanisms, with minor variations according to the composition of each pollutant or degree of oxidation/functionalization of the adsorbent. Such variations result in inferences about the mechanisms that are possibly most significant. However, only two studies bring this discussion among the works evaluating pesticide removal. Zhang et al., (2015a) briefly presented the possible mechanisms that influence the results obtained for different triazine pesticides in cellulose/graphene composite, concluding that it seems that van der Waals interactions are dominant in this specific case. On the other hand, Wang et al., (2019b) observed that for graphene/Fe_3O_4 nanocomposite, the possible adsorption mechanisms involved are an electrostatic attraction, hydrogen bonding interaction, hydrophobic interaction, and π–π stacking interaction. In this last work, the authors observed that graphene was the only component responsible for the adsorption since, individually, Fe_3O_4 was insignificant. In the case of drugs, it was estimated

that the removal of ketoprofen and norfloxacin in 3D GO with caffeic acid is related to electrostatic interaction, π–π interaction, and hydrogen bonds (Lu et al., 2020), but the removal of ciprofloxacin by three-dimensional porous graphene oxide-kaolinite-poly(vinyl alcohol) composite does not seem to be significantly related to electrostatic interactions (Huang et al., 2020). For endocrine disruptors, similar discussions are presented, and finally, the influence of material morphology is presented (Wang et al., 2019a). This morphology, although not discussed, can be understood as the high specific surface area and the porous structure attributed to these materials. Some articles also show that the π–π interaction is relevant for molecules containing conjugated six-membered rings, such as bisphenol A. At the same time, functional groups containing oxygen contribute to adsorption through hydrogen bonds (Chen et al., 2017a, b; Fang et al., 2018; Sun et al., 2019). Finally, no article evaluating hydrocarbon removal discusses the mechanisms involved in the process; however, it can be assumed that π–π interactions and material morphology are essential in this process.

For work with metals, many studies have used the X-ray photoelectron spectroscopy (XPS) technique to investigate the possible mechanisms of 3D metal–graphene interaction. This technique is widely applied due to the possibility of evaluating the chemical bonds that occur and monitoring the increase or decrease of specific bonds. This option is helpful in the case of metals, as the main mechanism is the chemical adsorption of metal ions through functional groups in 3D-graphene. This interaction takes place through electrostatic attraction, ion exchange, or chelation. A secondary mechanism mentioned is the physical adsorption that happens due to the porous structure and surface area of the adsorbents (Luo et al., 2020). For some metals, it can be inferred that the presence of certain groups in the adsorbents can optimize the adsorption process, as is the case of the presence of thiol groups in materials used in the removal of Hg(II) (Zhuang et al., 2018; Kabiri et al., 2016), Pb(II), and Cd(II) (Li et al., 2016; Wu et al., 2015; Yap et al., 2020), without disregarding the interaction with oxygenated and nitrogenous groups Chen et al., 2014b; Wu et al., 2015; Wang et al., 2017; Tan et al., 2018; Zhan et al., 2019). The presence of K^+ can help in the ion exchange process, being significant in the removal of Cs(I) (Huo et al., 2021) and Pb(II) (Liu et al., 2016). In some cases, the reduction of Cr(IV) to Cr(III), relatively more stable and less toxic, has also been described, followed by the formation of a chelate with –N or –O (Lei et al., 2014b; Wei et al., 2020). Finally, it was reported that the presence of defects on the surface of graphene, such as edges and vacancies, can help in the adsorption process (Huo et al., 2021), as well as the structure with open and interconnected pores also helps in the absorption of ions metallic, providing more spaces to immobilize and trap water pollutants within the micropores (Yap et al., 2020).

The mentioned adsorption mechanisms are already discussed in the literature, showing that controlling the composition, amount, and/or type of functional groups is essential to improve adsorption properties (Kong et al., 2021a). However, understanding how these factors specifically influence adsorption is not trivial. As an alternative, computer simulations have been increasingly used, which in addition to confirming the interpretations of experimental results concerning the adsorption capacity obtained (Firouzjaei et al., 2020) also allow the determination of the structure and properties of adsorbents even before the experiments (which saves time and financial resources) (Köhler et al., 2021). Thus, these simulations should be increasingly encouraged to understand these processes better, optimizing the experiments and bringing new mechanistic possibilities.

The main mechanisms in the experimental works can be summarized in morphology (i.e., surface area and pores) and chemical composition, including functional groups. We note two main points:

1. When a theory about the adsorption mechanisms is developed, the chemical composition is discussed, but the morphology is strongly neglected, resuming generic comments, which summarize good results to the presence of pores and large surface area. Here, we clearly observe that the adsorption is not directly related to the surface area; attributing good results to this factor seems imprecise.
2. In general, but specifically, the articles selected for this review do not show standardization regarding experimental parameters. Controlled experimental conditions are continually forgotten, and most articles do not even consider tem-

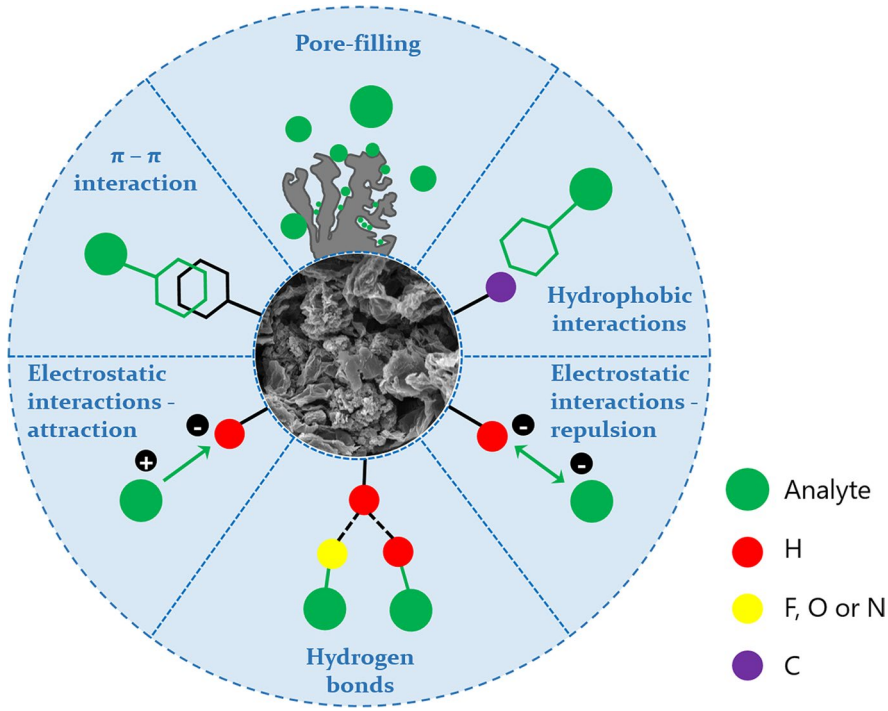

Fig. 6 Main adsorption mechanisms that are involved in the interaction of 3D graphene and analytes

perature and pH conditions, significantly limiting the discussion of their results.

9 Conclusions and Outlook

The three-dimensional structures based on graphene are objects of growing interest in different applications, standing out with promising adsorbents for emerging contaminants and other pollutants. These macrostructures have physical and chemical characteristics that allow removing these environmental interest molecules much higher than other conventional adsorbent materials. This better adsorption can be explained by different interaction mechanisms between the 3D based-graphene and the contaminant, mainly by π–π interaction, hydrogen bonds, and other hydrophobic interactions. In addition, 3D composites and functionalized materials can also interact with these pollutants through electrostatic interactions, which leads to higher selectivity and a broad range of contaminants that can be removed.

The absence of experimental standardization in the adsorption studies is observed among the studies reviewed in this work. Among the data summarized in Tables 1, 2, 3, 4, 5, and 6, it can be observed, for example, that part of the studies does not even provide information on the mass of material and volume of the analyte, making it impossible to determine the adsorbent dosage. At the same time, some studies show adsorptive capabilities for materials without presenting data on adsorption isotherms or contact time between the material and the analyte. In addition, part of the studies evaluates the influence of pH on the adsorption process. However, a significant portion does not take this parameter into account. Those parameters, such as the combination of correct analyte materials, seem more critical in removing contaminants than obtaining a material with a large specific surface area, but that does not present satisfactory interaction with the analyte. For this, it is essential to evaluate the material properties, such as the pH of the zero-charge point, which indicates the pH value that the surface of the material is neutral; hydrophobicity index; the presence of acidic and basic functional groups on the adsorbent surface; and, finally, the pore structure, since its diameter can act in the control of the adsorption process, preventing particles of larger diameters from penetrating the interior of the solid.

There is a wide variety of studies involving 3D graphene composites regarding their removal

efficiencies for different emerging pollutants and other contaminants such as dyes and heavy metal ions. However, a bottleneck in the application in natural systems of these 3D graphene materials is their large-scale production. Most of the studies cited in this review involve obtaining 3D materials on a laboratory scale, using high-purity reagents, methods involving several steps, high energy cost, often environmentally unfriendly routes, and difficulty in the size-controllable structure. Currently, these factors make the industrial-scale production of 3D graphene-based materials unviable. Further, several of these 3D materials still have poorly cohesive structures that can release small material fragments into the environment during the application, eventually becoming a nanocontaminant (da Rosa et al., 2021). This non-sustainability contrasts with the environmental application.

Composite formation and graphene functionalization have been alternatives in forming tightly connected networks, improving the material's mechanical properties, and sometimes making the material a multicomponent adsorbent. For there to be a real possibility of commercial applications of 3D graphene to remove contaminants, some challenges need to be overcome: it is necessary to understand the mechanisms involving the formation of these 3D graphene networks and how they interact with the pollutants. In this sense, the combination of theoretical and experimental studies has proved to be an inviting path. In addition, the effective cost of producing these materials must be attractive and, at the same time, coupled with production that is as sustainable as possible. There is still a lacking of literature on these two points. Thus, studies in this direction are essential to provide data for the commercialization and application of these graphene-based three-dimensional structures.

Funding The study was financially supported by the Brazilian National Council for Scientific and Technological Development (CNPq), the Research Support Foundation of the State of Rio Grande do Sul (FAPERGS) (21/2551–0002024-5), the Brazilian agency CNPq (424146/2018–5), FAPERGS (21/2551–0000736-2), and the National Institute of Science and Technology of carbon nanomaterials (INCT-Nanocarbon). This work was carried out with the support of the Coordination for the Improvement of Higher Education Personnel, Brazil (CAPES)—Financing Code 001.

Data Availability The datasets generated during and/or analyzed during the current study are available from the corresponding author upon reasonable request.

Declarations

Conflict of Interest The authors declare no competing interests.

References

Abouian Jahromi, M., Jamshidi-Zanjani, V., & Khodadadi Darban, A. (2020). Heavy metal pollution and human health risk assessment for exposure to surface soil of mining area: A comprehensive study. *Environmental Earth Sciences, 79*, 1–18.

Abu-Nada, A., McKay, G., & Abdala, A. (2020). Recent advances in applications of hybrid graphene materials for metals removal from wastewater. *Nanomaterials, 10*, 595.

Agathokleous, E., Barceló, D., Tsatsakis, A., & Calabrese, E. J. (2020). Hydrocarbon-induced hormesis: 101 years of evidence at the margin? *Environmental Pollution, 265*, 114846.

Ali, I., Alharbi, O. M., Tkachev, A., Galunin, E., Burakov, A., & Grachev, V. A. (2018). Water treatment by new-generation graphene materials: Hope for bright future. *Environmental Science and Pollution Research, 25*, 7315–7329.

Ali, I., ALOthman, Z. A., & Sanagi, M. M. (2015). Green synthesis of iron nano-impregnated adsorbent for fast removal of fluoride from water. *Journal of Molecular Liquids, 211*, 457–465.

Allen, M. J., Tung, V. C., & Kaner, R. B. (2010). Honeycomb carbon: A review of graphene. *Chemical Reviews, 110*, 132–145.

Almeida, C. A., de Oliveira, A. F., Pacheco, A. A., Lopes, R. P., Neves, A. A., & de Queiroz, M. E. L. R. (2018). Characterization and evaluation of sorption potential of the iron mine waste after Samarco dam disaster in Doce River basin–Brazil. *Chemosphere, 209*, 411–420.

Almeida, IMd., Jackson Filho, J. M., & Vilela, RAd. G. (2019). Razões para investigar a dimensão organizacional nas origens da catástrofe industrial da Vale em Brumadinho, Minas Gerais, Brasil. *Cadernos De Saúde Pública, 35*, e00027319.

Amini, A., Khajeh, M., Oveisi, A. R., Daliran, S., Ghaffari-Moghaddam, M., & Delarami, H. S. (2021). A porous multifunctional and magnetic layered graphene oxide/3D mesoporous MOF nanocomposite for rapid adsorption of uranium (VI) from aqueous solutions. *Journal of Industrial and Engineering Chemistry, 93*, 322–332.

Ananthashankar, R. (2012). *Treatment of textile effluent containing reactive red 120 dye using advanced oxidation*. Master Degree, Dalhousie University, Halifax - Nova Scotia, Canada.

Andrade, M. B., Santos, T. R., Fernandes Silva, M., Vieira, M. F., Bergamasco, R., & Hamoudi, S. (2019). Graphene oxide impregnated with iron oxide nanoparticles for the removal of atrazine from the aqueous medium. *Separation Science and Technology, 54*, 2653–2670.

Aragay, G., Pino, F., & Merkoçi, A. (2012). Nanomaterials for sensing and destroying pesticides. *Chemical Reviews, 112*, 5317–5338.

Asghar, F., Shakoor, B., Fatima, S., Munir, S., Razzaq, H., Naheed, S., & Butler, I. S. (2022). Fabrication and prospective applications of graphene oxide-modified nanocomposites for wastewater remediation. *RSC Advances, 12*, 11750–11768.

Asif, M. B., Iftekhar, S., Maqbool, T., Paramanik, B. K., Tabraiz, S., Sillanpää M., & Zhang, Z. (2021). Two-dimensional nanoporous and lamellar membranes for water purification: reality or a myth?. *Chemical Engineering Journal*, *432*, 134335.

Bachmatiuk, A., Mendes, R. G., Hirsch, C., Jähne, C., Lohe, M. R., Grothe, J., Kaskel, S., Fu, L., Klingeler, Rd., & Eckert, Jr. (2013). Few-layer graphene shells and nonmagnetic encapsulates: A versatile and nontoxic carbon nanomaterial. *ACS Nano, 7*, 10552–10562.

Bagoole, O., Rahman, M. M., Shah, S., Hong, H., Chen, H., Al Ghaferi, A., & Younes, H. (2018). Functionalized three-dimensional graphene sponges for highly efficient crude and diesel oil adsorption. *Environmental Science and Pollution Research, 25*, 23091–23105.

Bano, Z., Mazari, S. A., Saeed, R. Y., Majeed, M. A., Xia, M., Memon, A. Q., Abro, R., & Wang, F. (2020). Water decontamination by 3D graphene based materials: A review. *Journal of Water Process Engineering, 36*, 101404.

Beitollai, H., Safaei, M., & Tajik, S. (2019). Application of Graphene and Graphene Oxide for modification of electrochemical sensors and biosensors: A review. *International Journal of Nano Dimension, 10*, 125–140.

Bezerra, J. D., dos Santos Amaral, R., dos Santos Júnior, J. A., Genezini, F. A., Menezes, R. S. C., & de Oliveira, I. A. (2014). Characterization of heavy metals in a uranium ore region of the State of Pernambuco, Brazil. *Bulletin of Environmental Contamination and Toxicology, 92*, 270–273.

Bodzek, M., Konieczny, K., & Kwiecińska-Mydlak, A. (2020). Nanotechnology in water and wastewater treatment. Graphene–the nanomaterial for next generation of semipermeable membranes. *Critical Reviews in Environmental Science and Technology, 50*, 1515–1579.

Bong, J., Lim, T., Seo, K., Kwon, C.-A., Park, J. H., Kwak, S. K., & Ju, S. (2015). Dynamic graphene filters for selective gas-water-oil separation. *Scientific Reports, 5*, 14321.

Bose, S., & Drzal, L. T. (2015). Functionalization of graphene nanoplatelets using sugar azide for graphene/epoxy nanocomposites. *Carbon Letters, 16*(2), 101–106.

Brasileira, Q. (2017). *Borohidreto de Sódio*. Available in: https://www.quimicabrasileira.com.br/wp-content/uploads/2018/06/BOROHIDRETO-DE-SODIO-PA.pdf

Bryning, M. B., Milkie, D. E., Islam, M. F., Hough, L. A., Kikkawa, J. M., & Yodh, A. G. (2007). Carbon nanotube aerogels. *Advanced Materials, 19*, 661–664.

Burritt, R. L., & Christ, K. L. (2018). Water risk in mining: Analysis of the Samarco dam failure. *Journal of Cleaner Production, 178*, 196–205.

Cao, X., Yin, Z., & Zhang, H. (2014). Three-dimensional graphene materials: Preparation, structures and application in supercapacitors. *Energy & Environmental Science, 7*, 1850–1865.

Cargnelutti, F., Di Nisio, A., Pallotti, F., Sabovic, I., Spaziani, M., Tarsitano, M. G., Paoli, D., & Foresta, C. (2020). Effects of endocrine disruptors on fetal testis development, male puberty, and transition age. *Endocrine*, *72*,358–374.

Carrillo, B., Da Mata, D., Emanuel, L., Lopes, D., & Sampaio, B. (2019). Avoidable environmental disasters and infant health: Evidence from a mining dam collapse in Brazil. *Health Economics, 29*,1786–1794.

Chen, Z., Ren, W., Gao, L., Liu, B., Pei, S., & Cheng, H. M. (2011). Three-dimensional flexible and conductive interconnected graphene networks grown by chemical vapour deposition. *Nature Materials, 10*, 424–428.

Chen, C., Li, R., Xu, L., & Yan, D. (2014a). Three-dimensional superhydrophobic porous hybrid monoliths for effective removal of oil droplets from the surface of water. *RSC Advances, 4*, 17393–17400.

Chen, F., An, W., Liu, L., Liang, Y., & Cui, W. (2017a). Highly efficient removal of bisphenol A by a three-dimensional graphene hydrogel-AgBr@rGO exhibiting adsorption/photocatalysis synergy. *Applied Catalysis B: Environmental, 217*, 65–80.

Chen, G., Liu, Y., Liu, F., & Zhang, X. (2014b). Fabrication of three-dimensional graphene foam with high electrical conductivity and large adsorption capability. *Applied Surface Science, 311*, 808–815.

Chen, L., Li, Y., Du, Q., Wang, Z., Xia, Y., Yedinak, E., Lou, J., & Ci, L. (2017b). High performance agar/graphene oxide composite aerogel for methylene blue removal. *Carbohydrate Polymers, 155*, 345–353.

Chen, Y., Chen, L., Bai, H., & Li, L. (2013a). Graphene oxide–chitosan composite hydrogels as broad-spectrum adsorbents for water purification. *Journal of Materials Chemistry A, 1*, 1992–2001.

Chen, Y., Song, X., Zhao, T., Xiao, Y., Wang, Y., & Chen, X. (2018). A phosphorylethanolamine-functionalized superhydrophilic 3D graphene-based foam filter for water purification. *Journal of Hazardous Materials, 343*, 298–303.

Chen, Y., Star, A., & Vidal, S. (2013b). Sweet carbon nanostructures: Carbohydrate conjugates with carbon nanotubes and graphene, and their applications. *Chemical Society Reviews, 42*, 4532–4542.

Chen, Y., Zhang, Q., Chen, L., Bai, H., & Li, L. (2013c). Basic aluminum sulfate@ graphene hydrogel composites: Preparation and application for removal of fluoride. *Journal of Materials Chemistry A, 1*, 13101–13110.

Cheng, J.-S., Du, J., & Zhu, W. (2012). Facile synthesis of three-dimensional chitosan–graphene mesostructures for reactive black 5 removal. *Carbohydrate Polymers, 88*, 61–67.

Cordeiro, M. C., Garcia, G. D., Rocha, A. M., Tschoeke, D. A., Campeão, M. E., Appolinario, L. R., Soares, A. C., Leomil, L., Froes, A., & Bahiense, L. (2019). Insights on the freshwater microbiomes metabolic changes associated with the world's largest mining disaster. *Science of the Total Environment, 654*, 1209–1217.

Da Rosa, P. C. C., Leão, M. B., Dalla Corte, C. L., & de Matos, C. F. (2021). Evaluation of the Carbon Nanostructures Toxicity as a Function of Their Dimensionality Using

Model Organisms: A Review. *Water, Air, & Soil Pollution, 232*, 1–15.

Da'na, E. (2017). Adsorption of heavy metals on functionalized-mesoporous silica: A review. *Microporous and Mesoporous Materials, 247*, 145–157.

Dang, Z., & Kienzler, A. (2019). Changes in fish sex ratio as a basis for regulating endocrine disruptors. *Environment International, 130*, 104928.

Darbre, P. D. (2017). Endocrine disruptors and obesity. *Current Obesity Reports, 6*, 18–27.

de Souza, P. A. (2019). Open data could have helped us learn from another mining dam disaster. *Scientific Data, 6*, 1–2.

Deng, J., Lei, B., He, A., Zhang, X., Ma, L., Li, S., & Zhao, C. (2013). Toward 3D graphene oxide gels based adsorbents for high-efficient water treatment via the promotion of biopolymers. *Journal of Hazardous Materials, 263*, 467–478.

Edwards, D. P., & Laurance, W. F. (2015). Preventing tropical mining disasters. *Science, 350*, 1482–1482.

Eliasson, J. (2015). The rising pressure of global water shortages. *Nature, 517*, 6–6.

Erbil, H. Y. (2021). Dependency of contact angles on three-phase contact line: A review. *Colloids and Interfaces, 5*, 8.

Fang, Q., & Chen, B. (2014). Self-assembly of graphene oxide aerogels by layered double hydroxides cross-linking and their application in water purification. *Journal of Materials Chemistry A, 2*, 8941–8951.

Fang, Q., Zhou, X., Deng, W., & Liu, Z. (2017). Hydroxyl-containing organic molecule induced self-assembly of porous graphene monoliths with high structural stability and recycle performance for heavy metal removal. *Chemical Engineering Journal, 308*, 1001–1009.

Fang, Z., Hu, Y., Wu, X., Qin, Y., Cheng, J., Chen, Y., Tan, P., & Li, H. (2018). A novel magnesium ascorbyl phosphate graphene-based monolith and its superior adsorption capability for bisphenol A. *Chemical Engineering Journal, 334*, 948–956.

Farzin, S., Chianeh, F. N., Anaraki, M. V., & Mahmoudian, F. (2020). Introducing a framework for modeling of drug electrochemical removal from wastewater based on data mining algorithms, scatter interpolation method, and multi criteria decision analysis (DID). *Journal of Cleaner Production, 266*, 122075.

Feng, J., Ye, Y. Xiao, M., Wu G., & Ke, Y. (2020). Synthetic routes of the reduced graphene oxide. *Chemical Papers, 74,* 3767–3783.

Firouzjaei, M. D., Afkhami, F. A., Esfahani, M. R., Turner, C. H., & Nejati, S. (2020). Experimental and molecular dynamics study on dye removal from water by a graphene oxide-copper-metal organic framework nanocomposite. *Journal of Water Process Engineering, 34*, 101180.

Freitas, CMd., Barcellos, C., Asmus, C. I. R. F., Silva, MAd., & Xavier, D. R. (2019a). Da Samarco em Mariana à Vale em Brumadinho: desastres em barragens de mineração e Saúde Coletiva. *Cadernos de Saúde Pública, 35*, e00052519.

Freitas, CMd., Barcellos, C., Heller, L., & Luz, Z. MPd. (2019b). Desastres em barragens de mineração: Lições do passado para reduzir riscos atuais e futuros. *Epidemiologia e Serviços De Saúde, 28*, e20180120.

Gao, H., Sun, Y., Zhou, J., Xu, R., & Duan, H. (2013). Mussel-inspired synthesis of polydopamine-functionalized graphene hydrogel as reusable adsorbents for water purification. *ACS Applied Materials & Interfaces, 5*(2), 425–432.

Garcia, L. C., Ribeiro, D. B., de Oliveira Roque, F., Ochoa-Quintero, J. M., & Laurance, W. F. (2017). Brazil's worst mining disaster: Corporations must be compelled to pay the actual environmental costs. *Ecological Applications, 27*, 5–9.

Geim, A. K. (2009). Graphene: Status and prospects. *Science, 324*, 1530–1534.

Gomes, L., Chippari-Gomes, A., Miranda, T., Pereira, T., Merçon, J., Davel, V., Barbosa, B., Pereira, A., Frossard, A., & Ramos, J. (2019). Genotoxicity effects on Geophagus brasiliensis fish exposed to Doce River water after the environmental disaster in the city of Mariana, MG, Brazil. *Brazilian Journal of Biology, 79*, 659–664.

Guan, L.-Z., Zhao, L., Wan, Y.-J., & Tang, L.-C. (2018). Three-dimensional graphene-based polymer nanocomposites: Preparation, properties and applications. *Nanoscale, 10*, 14788–14811.

Guardian, T. (2018). *Brazil dam disaster: firm knew of potential impact months in advance*. Available in: https://www.theguardian.com/world/2018/feb/28/brazil-dam-collapse-samarco-fundao-mining

Guo, X., Qu, L., Zhu, S., Tian, M., Zhang, X., Sun, K., & Tang, X. (2016). Preparation of three-dimensional chitosan–graphene oxide aerogel for residue oil removal. *Water Environment Research, 88*, 768–778.

Han, Z., Tang, Z., Shen, S., Zhao, B., Zheng, G., & Yang, J. (2014). Strengthening of graphene aerogels with tunable density and high adsorption capacity towards Pb^{2+}. *Scientific Reports, 4*, 5025.

Hassaan, M. A., & El Nemr, A. (2017). Advanced oxidation processes for textile wastewater treatment. *International Journal of Photochemistry and Photobiology, 2*, 85–93.

Heller, L. (2019). Desastres en la minería y la salud pública en Brasil: lecciones (no) aprendidas. *SciELO Public Health, 35*, e00073619.

Hiew, B. Y. Z., Lee, L. Y., Lee, X. J., Thangalazhy-Gopakumar, S., Gan, S., Lim, S. S., Pan, G.-T., Yang, T.C.-K., Chiu, W. S., & Khiew, P. S. (2018). Review on synthesis of 3D graphene-based configurations and their adsorption performance for hazardous water pollutants. *Process Safety and Environmental Protection, 116*, 262–286.

Hou, P., Xing, G., Han, D., Wang, H., Yu, C., & Li, Y. (2018). Preparation of zeolite imidazolate framework/graphene hybrid aerogels and their application as highly efficient adsorbent. *Journal of Solid State Chemistry, 265*, 184–192.

Hu, H., Zhao, Z., Wan, W., Gogotsi, Y., & Qiu, J. (2013). Ultralight and highly compressible graphene aerogels. *Advanced Materials, 25*, 2219–2223.

Hu, C., Grant, D., Hou, X., & Xu, F. (2021). High rhodamine B and methyl orange removal performance of graphene oxide/carbon nanotube nanostructures. *Materials Today: Proceedings, 34*, 184–193.

Huang, X., Tian, J., Li, Y., Yin, X., & Wu, W. (2020). Preparation of a Three-Dimensional Porous Graphene

Oxide–Kaolinite–Poly (vinyl alcohol) Composite for Efficient Adsorption and Removal of Ciprofloxacin. *Langmuir, 36*, 10895–10904.

Huang, Y., Li, C., & Lin, Z. (2014). EDTA-induced self-assembly of 3D graphene and its superior adsorption ability for paraquat using a teabag. *ACS Applied Materials & Interfaces, 6*, 19766–19773.

Huo, J., Yu, G., & Wang, J. (2021). Selective adsorption of cesium (I) from water by Prussian blue analogues anchored on 3D reduced graphene oxide aerogel. *Science of the Total Environment, 761*, 143286.

Hussain, A., Alamzeb, S., & Begum, S. (2013). Accumulation of heavy metals in edible parts of vegetables irrigated with waste water and their daily intake to adults and children, District Mardan, Pakistan. *Food Chemistry, 136*, 1515–1523.

Iijima, S. (1991). Helical microtubules of graphitic carbon. *Nature, 354*, 56–58.

Huhtamäki, T., Tian, X., Korhonen, J. T., & Ras, R. H. (2018). Surface-wetting characterization using contact-angle measurements. *Nature Protocols, 13*, 1521–1538.

Ji, C.-C., Xu, M.-W., Bao, S.-J., Cai, C.-J., Lu, Z.-J., Chai, H., Yang, F., & Wei, H. (2013). Self-assembly of three-dimensional interconnected graphene-based aerogels and its application in supercapacitors. *Journal of Colloid and Interface Science, 407*, 416–424.

Jia, J., Sun, X., Lin, X., Shen, X., Mai, Y.-W., & Kim, J.-K. (2014). Exceptional electrical conductivity and fracture resistance of 3D interconnected graphene foam/epoxy composites. *ACS Nano, 8*, 5774–5783.

Jing, J., Qian, X., Si, Y., Liu, G., & Shi, C. (2022). Recent Advances in the Synthesis and Application of Three-Dimensional Graphene-Based Aerogels. *Molecules, 27*, 924.

Jones, S., Pramanik, A., Kanchanapally, R., Viraka Nellore, B. P., Begum, S., Sweet, C., & Ray, P. C. (2017). Multifunctional three-dimensional chitosan/gold nanoparticle/graphene oxide architecture for separation, label-free SERS identification of pharmaceutical contaminants, and effective killing of superbugs. *ACS Sustainable Chemistry & Engineering, 5*, 7175–7187.

Kabiri, S., Tran, D. N., Cole, M. A., & Losic, D. (2016). Functionalized three-dimensional (3D) graphene composite for high efficiency removal of mercury. *Environmental Science: Water Research Technology, 2*, 390–402.

Kasap, S. (2020). Development of foamy-like 3-dimensional graphene networks decorated with iron oxide nanoparticles for strontium adsorption. *Separation Science and Technology, 56*, 1184–1194.

Kim, M. S., Fang, B., Kim, J. H., Yang, D., Kim, Y. K., Bae, T. S., & Yu, J. S. (2011). Ultra-high Li storage capacity achieved by hollow carbon capsules with hierarchical nanoarchitecture. *Journal of Materials Chemistry, 21*, 19362–19367.

Köhler, M. H., Bordin, J. R., & Barbosa, M. C. (2018). 2D nanoporous membrane for cation removal from water: Effects of ionic valence, membrane hydrophobicity, and pore size. *The Journal of Chemical Physics, 148*, 222804.

Köhler, M. H., Bordin, J. R., & Barbosa, M. C. (2019a). Ion flocculation in water: From bulk to nanoporous membrane desalination. *Journal of Molecular Liquids, 277*, 516–521.

Köhler, M. H., Bordin, J. R., de Matos, C. F., & Barbosa, M. C. (2019b). Water in nanotubes: The surface effect. *Chemical Engineering Science, 203*, 54–67.

Köhler, M. H., Leão, M. B., Bordin, J. R., & Matos, C. F. d. (2021). Three-Dimensional and Lamellar Graphene Oxide Membranes for Water Purification. In: *Two-Dimensional (2D) Nanomaterials in Separation Science* (p 87–111), Springer.

Kong, Q., Shi, X., Ma, W., Zhang, F., Yu, T., Zhao, F., Zhao, D., & Wei, C. (2021a). Strategies to improve the adsorption properties of graphene-based adsorbent towards heavy metal ions and their compound pollutants: A review. *Journal of Hazardous Materials, 415*, 125690.

Kong, Y., Ji, C., Qu, J., Chen, Y., Wu, S., Zhu, X., Niu, L., & Zhao, M. (2021b). Old pesticide, new use: Smart and safe enantiomer of isocarbophos in locust control. *Ecotoxicology and Environmental Safety, 225*, 112710.

Kumar, A., Kumar, A., Cabral-Pinto, M. M. S., Chaturvedi, A. K., Shabnam, A. A., Subrahmanyam, G., Mondal, R., Gupta, D. K., Malyan, S. K., & Kumar, S. S. (2020). Lead toxicity: health hazards, influence on food chain, and sustainable remediation approaches. *International Journal of Environmental Research And Public Health, 17*, 2179.

Labonne, B. (2016). Mining dam failure: Business as usual? *The Extractive Industries and Society, 3*, 651–652.

Leão, M. B., da Rosa, P. C. C., Dalla Corte, C. L., & Matos, CFd. (2022). Eco-friendly, non-toxic and super adsorbent hydrogels based on graphene. *Materials Chemistry and Physics, 288*, 126408.

Leão, M. B., Gonçalves, D. F., Miranda, G. M., da Paixão, G. M., & Dalla Corte, C. L. (2019). Toxicological evaluation of the herbicide Palace® in *Drosophila melanogaster*. *Journal of Toxicology and Environmental Health, Part A, 82*, 1172–1185.

Lee, C. S. L., Li, X., Shi, W., Cheung, S. C. N., & Thornton, I. (2006). Metal contamination in urban, suburban, and country park soils of Hong Kong: a study based on GIS and multivariate statistics. *Science of the Total Environment, 356*, 45–61.

Lee, K. G., Jeong, J.-M., Lee, S. J., Yeom, B., Lee, M.-K., & Choi, B. G. (2015). Sonochemical-assisted synthesis of 3D graphene/nanoparticle foams and their application in supercapacitor. *Ultrasonics Sonochemistry, 22*, 422–428.

Lei, Y., Chen, F., Luo, Y., & Zhang, L. (2014a). Synthesis of three-dimensional graphene oxide foam for the removal of heavy metal ions. *Chemical Physics Letters, 593*, 122–127.

Lei, Y., Chen, F., Luo, Y., & Zhang, L. (2014b). Three-dimensional magnetic graphene oxide foam/Fe_3O_4 nanocomposite as an efficient absorbent for Cr (VI) removal. *Journal of Materials Science, 49*, 4236–4245.

Li, C., Zhou, K., Qin, W., Tian, C., Qi, M., Yan, X., & Han, W. (2019). A review on heavy metals contamination in soil: Effects, sources, and remediation techniques. *Soil and Sediment Contamination: An International Journal, 28*, 380–394.

Li, F., Wang, X., Yuan, T., & Sun, R. (2016). A lignosulfonate-modified graphene hydrogel with ultrahigh adsorption

capacity for Pb (II) removal. *Journal of Materials Chemistry A, 4*, 11888–11896.

Li, W., Gao, S., Wu, L., Qiu, S., Guo, Y., Geng, X., Chen, M., Liao, S., Zhu, C., & Gong, Y. (2013). High-density three-dimension graphene macroscopic objects for high-capacity removal of heavy metal ions. *Scientific Reports, 3*, 2125.

Liao, C., Zhao, X.-R., Jiang, X.-Y., Teng, J., & Yu, J.-G. (2020). Hydrothermal fabrication of novel three-dimensional graphene oxide-pentaerythritol composites with abundant oxygen-containing groups as efficient adsorbents. *Microchemical Journal, 152*, 104288.

Lim, J. Y., Mubarak, N., Abdullah, E., Nizamuddin, S., & Khalid, M. (2018). Recent trends in the synthesis of graphene and graphene oxide based nanomaterials for removal of heavy metals – A review. *Journal of Industrial and Engineering Chemistry, 66*, 29–44.

Lin, Y., Tian, Y., Sun, H., & Hagio, T. (2021). Progress in modifications of 3D graphene-based adsorbents for environmental applications. *Chemosphere, 270*, 129420.

Liu, F., Chung, S., Oh, G., & Seo, T. S. (2012). Three-dimensional graphene oxide nanostructure for fast and efficient water-soluble dye removal. *ACS Applied Materials & Interfaces, 4*(2), 922–927.

Liu, H., & Qiu, H. (2020). Recent advances of 3D graphene-based adsorbents for sample preparation of water pollutants: A review. *Chemical Engineering Journal, 393*, 124691.

Liu, C., Liu, H., Xu, A., Tang, K., Huang, Y., & Lu, C. (2017a). In situ reduced and assembled three-dimensional graphene aerogel for efficient dye removal. *Journal of Alloys and Compounds, 714*, 522–529.

Liu, H., Wang, X., Ding, C., Dai, Y., Sun, Y., Lin, Y., Sun, W., Zhu, X., Han, R., & Gao, D. (2019a). Carboxylated carbon nanotubes-graphene oxide aerogels as ultralight and renewable high performance adsorbents for efficient adsorption of glyphosate. *Environmental Chemistry, 17*, 6–16.

Liu, J., Ge, X., Ye, X., Wang, G., Zhang, H., Zhou, H., Zhang, Y., & Zhao, H. (2016). 3D graphene/δ-MnO_2 aerogels for highly efficient and reversible removal of heavy metal ions. *Journal of Materials Chemistry A, 4*, 1970–1979.

Liu, S., Yao, F., Oderinde, O., Zhang, Z., & Fu, G. (2017b). Green synthesis of oriented xanthan gum–graphene oxide hybrid aerogels for water purification. *Carbohydrate Polymers, 174*, 392–399.

Liu, X., Bai, Z., Shi, H., Zhou, W., & Liu, X. (2019b). Heavy metal pollution of soils from coal mines in China. *Natural Hazards, 99*, 1163–1177.

Liu, X.-L., Wang, C., Wu, Q.-H., & Wang, Z. (2014). Preconcentration of chlorophenols in water samples using three-dimensional graphene-based magnetic nanocomposite as absorbent. *Chinese Chemical Letters, 25*, 1185–1189.

Liu, Y., Xiang, M., & Hong, L. (2017c). Three-dimensional nitrogen and boron codoped graphene for carbon dioxide and oils adsorption. *RSC Advances, 7*, 6467–6473.

Lu, Y., Li, Y., Gao, Y., Ai, B., Gao, W., & Peng, G. (2020). Facile preparation of 3D GO with caffeic acid for efficient adsorption of norfloxacin and ketoprofen. *Water Science and Technology, 81*, 1461–1470.

Luo, J., Fan, C., & Zhou, X. (2021a). Functionalized graphene oxide/carboxymethyl chitosan composite aerogels with strong compressive strength for water purification. *Journal of Applied Polymer Science, 138*, 50065.

Luo, J., Fu, K., Yu, D., Hristovski, K. D., Westerhoff, P., & Crittenden, J. C. (2021b). Review of Advances in Engineering Nanomaterial Adsorbents for Metal Removal and Recovery from Water: Synthesis and Microstructure Impacts. *ACS ES&T Engineering, 1*, 623–661.

Luo, Z., Li, D., Huang, L., Tan, S., & Huang, J. (2020). Flexible and superhydrophobic aerogel based on an interpenetrating network of konjac glucomannan and reduced graphene oxide for efficient water–oil separation. *Journal of Materials Science, 55*, 12884–12896.

Ma, Y., & Zhi, L. (2021). Functionalized graphene materials: Definition, classification, and preparation strategies. *Acta Physico-Chimica Sinica, 37*, 3866.

Ma, J., Yang, M., Yu, F., & Zheng, J. (2015). Water-enhanced removal of ciprofloxacin from water by porous graphene hydrogel. *Scientific Reports, 5*, 13578.

Ma, T., Chang, P. R., Zheng, P., Zhao, F., & Ma, X. (2014). Fabrication of ultra-light graphene-based gels and their adsorption of methylene blue. *Chemical Engineering Journal, 240*, 595–600.

Ma, Y.-X., Li, X., Shao, W.-J., Kou, Y.-L., Yang, H.-P., & Zhang, D.-J. (2020). Fabrication of 3D porous polyvinyl alcohol/sodium alginate/graphene oxide spherical composites for the adsorption of methylene blue. *Journal of Nanoscience and Nanotechnology, 20*, 2205–2213.

Mackuľak, T., Nagyova, K., Faberova, M., Grabic, R., Koba, O., Gal, M., & Birošová, L. (2015). Utilization of Fenton-like reaction for antibiotics and resistant bacteria elimination in different parts of WWTP. *Environmental Toxicology and Pharmacology, 40*, 492–497.

Mahpishanian, S., & Sereshti, H. (2016). Three-dimensional graphene aerogel-supported iron oxide nanoparticles as an efficient adsorbent for magnetic solid phase extraction of organophosphorus pesticide residues in fruit juices followed by gas chromatographic determination. *Journal of Chromatography A, 1443*, 43–53.

Majumder, P., & Gangopadhyay, R. (2022). Evolution of graphene oxide (GO)-based nanohybrid materials with diverse compositions: An overview. *RSC Advances, 12*, 5686–5719.

Maliyekkal, S. M., Sreeprasad, T. S., Krishnan, D., Kouser, S., Mishra, A. K., Waghmare, U. V., & Pradeep, T. (2013). Graphene: a reusable substrate for unprecedented adsorption of pesticides. *Small, 9*, 273–283.

Mao, C., Song, Y., Chen, L., Ji, J., Li, J., Yuan, X., Yang, Z., Ayoko, G. A., Frost, R. L., & Theiss, F. (2019). Human health risks of heavy metals in paddy rice based on transfer characteristics of heavy metals from soil to rice. *CATENA, 175*, 339–348.

Mauter, M. S., & Elimelech, M. (2008). Environmental applications of carbon-based nanomaterials. *Environmental Science & Technology, 42*, 5843–5859.

Meng, Y., Wang, K., Zhang, Y., & Wei, Z. (2013). Hierarchical porous graphene/polyaniline composite film with superior rate performance for flexible supercapacitors. *Advanced Materials, 25*, 6985–6990.

Mu, C., Zhang, Y., Cui, W., Liang, Y., & Zhu, Y. (2017). Removal of bisphenol A over a separation free 3D Ag_3PO_4-graphene hydrogel via an adsorption-photocatalysis synergy. *Applied Catalysis B: Environmental, 212*, 41–49.

Munhoz, L. (2019). The Brazilian Brumadinho Mining Disaster: Environmental Regulation on Debate. *Natural Resources & Environment, 34*, 37–41.

Nardecchia, S., Carriazo, D., Ferrer, M. L., Gutiérrez, M. C., & del Monte, F. (2013). Three dimensional macroporous architectures and aerogels built of carbon nanotubes and/or graphene: Synthesis and applications. *Chemical Society Reviews, 42*, 794–830.

Nguyen, H. N., Chenoweth, J. A., Bebarta, V. S., Albertson, T. E., & Nowadly, C. D. (2021). The toxicity, pathophysiology, and treatment of acute hydrazine propellant exposure: A systematic review. *Military Medicine, 186*, e319–e326.

Noal, Dd. S., Rabelo, I. V. M., & Chachamovich, E. (2019). O impacto na saúde mental dos afetados após o rompimento da barragem da Vale. *Cadernos de Saúde Pública, 35*, e00048419.

Nodeh, H. R., Kamboh, M. A., Ibrahim, W. A. W., Jume, B. H., Sereshti, H., & Sanagi, M. M. (2019). Equilibrium, kinetic and thermodynamic study of pesticides removal from water using novel glucamine-calix [4] arene functionalized magnetic graphene oxide. *Environmental Science: Processes & Impacts, 21*, 714–726.

Novoselov, K. S., Geim, A. K., Morozov, S. V., Jiang, D., Zhang, Y., Dubonos, S. V., Grigorieva, I. V., & Firsov, A. A. (2004). Electric field effect in atomically thin carbon films. *Science, 306*, 666–669.

Oğuz, M., & Mihçiokur, H. (2014). Environmental risk assessment of selected pharmaceuticals in Turkey. *Environmental Toxicology and Pharmacology, 38*, 79–83.

Oliveira, V. G., Tolentino, N. M., & de Oliveira, P. H. R. (2015). Hidrazina (CAS 302–01-2). *Revista Virtual De Química, 7*, 1570–1578.

Owen, J., Kemp, D., Lèbre, É., Svobodova, K., & Murillo, G. P. (2020). Catastrophic tailings dam failures and disaster risk disclosure. *International Journal of Disaster Risk Reduction, 42*, 101361.

Pan, L., Liu, S., Oderinde, O., Li, K., Yao, F., & Fu, G. (2018). Facile fabrication of graphene-based aerogel with rare earth metal oxide for water purification. *Applied Surface Science, 427*, 779–786.

Park, H. S., & Kang, S. O. (2016). Sorption behavior of slightly reduced, three-dimensionally macroporous graphene oxides for physical loading of oils and organic solvents. *Carbon Letters, 18*, 24–29.

Passaretti, P. (2022). Graphene Oxide and Biomolecules for the Production of Functional 3D Graphene-Based Materials. *Frontiers in Molecular Biosciences, 9*, 774097.

Peng, H.-J., Liang, J., Zhu, L., Huang, J.-Q., Cheng, X.-B., Guo, X., Ding, W., Zhu, W., & Zhang, Q. (2014). Catalytic self-limited assembly at hard templates: A mesoscale approach to graphene nanoshells for lithium–sulfur batteries. *ACS Nano, 8*, 11280–11289.

Peng, T., Lv, H., He, D., Pan, M., & Mu, S. (2013). Direct transformation of amorphous silicon carbide into graphene under low temperature and ambient pressure. *Scientific Reports, 3*, 1–7.

Power, A., Chandra, S., & Chapman, J. (2018). Graphene, electrospun membranes and granular activated carbon for eliminating heavy metals, pesticides and bacteria in water and wastewater treatment processes. *The Analyst, 143*, 5629–5645.

Qi, X., Pu, K. Y., Zhou, X., Li, H., Liu, B., Boey, F., Huang, W., & Zhang, H. (2010). Conjugated-polyelectrolyte-functionalized reduced graphene oxide with excellent solubility and stability in polar solvents. *Small, 6*, 663–669.

Queiroz, H. M., Nóbrega, G. N., Ferreira, T. O., Almeida, L. S., Romero, T. B., Santaella, S. T., Bernardino, A. F., & Otero, X. L. (2018). The Samarco mine tailing disaster: A possible time-bomb for heavy metals contamination? *Science of the Total Environment, 637*, 498–506.

Rancière, F., Botton, J., Slama, R., Lacroix, M. Z., Debrauwer, L., Charles, M. A., Roussel, R., Balkau, B., Magliano, D. J., & D.E.S.I.R. Study Group. (2019). Exposure to Bisphenol A and Bisphenol S and Incident Type 2 Diabetes: A case-cohort study in the French Cohort DESIR. *Environmental Health Perspectives, 127*, 107013.

Rani, L., Thapa, K., Kanojia, N., Sharma, N., Singh, S., Grewal, A. S., Srivastav, A. L., & Kaushal, J. (2021). An extensive review on the consequences of chemical pesticides on human health and environment. *Journal of Cleaner Production, 283*, 124657.

Rao, CeNe. R., Sood, Ae. K., Subrahmanyam, Ke. S., & Govindaraj, A. (2009). Graphene: the new two-dimensional nanomaterial. *Angewandte Chemie International Edition, 48*, 7752–7777.

Rico, M., Benito, G., Salgueiro, A. R., Díez-Herrero, A., & Pereira, H. G. (2008). Reported tailings dam failures: a review of the European incidents in the worldwide context. *Journal of Hazardous Materials, 152*, 846–852.

Roche, C., Thygesen, K., & Baker, E. (2017). Mine tailings storage: safety is no accident, A UNEP Rapid Response Assessment. *United Nations Environment Programme and GRID-Arendal, Nairobi and Arendal*. Available in: https://www.grida.no/publications/383

Santamarina, J. C., Torres-Cruz, L. A., & Bachus, R. C. (2019). Why coal ash and tailings dam disasters occur. *Science, 364*, 526–528.

Santos, T. R., Andrade, M. B., Silva, M. F., Bergamasco, R., & Hamoudi, S. (2019). Development of α-and γ-Fe2O3 decorated graphene oxides for glyphosate removal from water. *Environmental Technology, 40*, 1118–1137.

Shan, D., Deng, S., Jiang, C., Chen, Y., Wang, B., Wang, Y., Huang, J., Yu, G., & Wiesner, M. R. (2018). Hydrophilic and strengthened 3D reduced graphene oxide/nano-Fe_3O_4 hybrid hydrogel for enhanced adsorption and catalytic oxidation of typical pharmaceuticals. *Environmental Science: Nano, 5*, 1650–1660.

Shen, Y., Fang, Q., & Chen, B. (2015). Environmental applications of three-dimensional graphene-based macrostructures: Adsorption, transformation, and detection. *Environmental Science & Technology, 49*, 67–84.

Shu, D., Feng, F., Han, H., & Ma, Z. (2017). Prominent adsorption performance of amino-functionalized ultra-light

graphene aerogel for methyl orange and amaranth. *Chemical Engineering Journal, 324*, 1–9.

Siviter, H., Bailes, E. J., Martin, C. D., Oliver, T. R., Koricheva, J., Leadbeater, E., & Brown, M. J. (2021). Agrochemicals interact synergistically to increase bee mortality. *Nature, 596*, 389–392.

Smith, A. T., LaChance, A. M., Zeng, S., Liu, B., & Sun, L. (2019). Synthesis, properties, and applications of graphene oxide/reduced graphene oxide and their nanocomposites. *Nano Materials Science, 1*, 31–47.

Solangi, N. H., Kumar, J., Mazari, S. A., Ahmed, S., Fatima, N., & Mubarak, N. M. (2021). Development of fruit waste derived bio-adsorbents for wastewater treatment: A review. *Journal of Hazardous Materials, 416*, 125848.

Song, J.-W., & Fan, L.-W. (2021). Temperature dependence of the contact angle of water: A review of research progress, theoretical understanding, and implications for boiling heat transfer. *Advances in Colloid and Interface Science, 288*, 102339.

Stoller, M. D., Park, S., Zhu, Y., An, J., & Ruoff, R. S. (2008). Graphene-based ultracapacitors. *Nano Letters, 8*, 3498–3502.

Sui, Z.-Y., Cui, Y., Zhu, J.-H., & Han, B.-H. (2013). Preparation of three-dimensional graphene oxide–polyethylenimine porous materials as dye and gas adsorbents. *ACS Applied Materials & Interfaces, 5*, 9172–9179.

Sun, Y., Wang, C., Xue, Y., Zhang, Q., Mendes, R. G., Chen, L., Zhang, T., Gemming, T., Rümmeli, M. H., & Ai, X. (2016). Coral-inspired nanoengineering design for long-cycle and flexible lithium-ion battery anode. *ACS Applied Materials & Interfaces, 8*, 9185–9193.

Sun, Z., Fang, S., & Hu, Y. H. (2020). 3D graphene materials: From understanding to design and synthesis control. *Chemical Reviews, 120*, 10336–10453.

Sun, Z., Zhao, L., Liu, C., Zhen, Y., Zhang, W., & Ma, J. (2019). A novel 3D adsorbent of reduced graphene oxide-β-cyclodextrin aerogel coupled hardness with softness for efficient removal of bisphenol A. *Chemical Engineering Journal, 372*, 896–904.

Tan, B., Zhao, H., Zhang, Y., Quan, X., He, Z., Zheng, W., & Shi, B. (2018). Amphiphilic PA-induced three-dimensional graphene macrostructure with enhanced removal of heavy metal ions. *Journal of Colloid and Interface Science, 512*, 853–861.

Tang, F. H., Lenzen, M., McBratney, A., & Maggi, F. (2021). Risk of pesticide pollution at the global scale. *Nature Geoscience, 14*, 206–210.

Tang, Z., Shen, S., Zhuang, J., & Wang, X. (2010). Noble-metal-promoted three-dimensional macroassembly of single-layered graphene oxide. *Angewandte Chemie, 122*, 4707–4711.

Tiwari, J. N., Mahesh, K., Le, N. H., Kemp, K. C., Timilsina, R., Tiwari, R. N., & Kim, K. S. (2013). Reduced graphene oxide-based hydrogels for the efficient capture of dye pollutants from aqueous solutions. *Carbon, 56*, 173–182.

Tkaczyk, A., Mitrowska, K., & Posyniak, A. (2020). Synthetic organic dyes as contaminants of the aquatic environment and their implications for ecosystems: A review. *Science of the Total Environment, 717*, 137222.

Tuncak, B. (2017). Lessons from the Samarco Disaster. *BHRJ, 2*, 157.

Umbreen, N., Sohni, S., Ahmad, I., Khattak, N. U., & Gul, K. (2018). Self-assembled three-dimensional reduced graphene oxide-based hydrogel for highly efficient and facile removal of pharmaceutical compounds from aqueous solution. *Journal of Colloid and Interface Science, 527*, 356–367.

Umemoto, K., Saito, S., Berber, S., & Tománek, D. (2001). Carbon foam: Spanning the phase space between graphite and diamond. *Physical Review B, 64*, 193409.

UNESCO. (2017). *The United Nations world water development report 2017. Wastewater: the untapped resource*. UNESCO Paris.

UNESCO. (2019). *The United Nations world water development report 2019: Leaving no one behind*. UNESCO Paris.

Velusamy, S., Roy, A., Sundaram, S., & Kumar Mallick, T. (2021). A review on heavy metal ions and containing dyes removal through graphene oxide-based adsorption strategies for textile wastewater treatment. *The Chemical Record, 21*, 1570–1610.

Verma, S., & Nadagouda, M. N. (2021). Graphene-Based Composites for Phosphate Removal. *ACS Omega, 6*, 4119–4125.

Vickery, J. L., Patil, A. J., & Mann, S. (2009). Fabrication of graphene–polymer nanocomposites with higher-order three-dimensional architectures. *Advanced Materials, 21*, 2180–2184.

Vieira, W. T., de Farias, M. B., Spaolonzi, M. P., da Silva, M. G. C., & Vieira, M. G. A. (2020). Removal of endocrine disruptors in waters by adsorption, membrane filtration and biodegradation. A review. *Environmental Chemistry Letters, 18*, 1113–1143.

Wang, F., Guan, Q., Tian, J., Lin, J., Yang, Y., Yang, L., & Pan, N. (2020a). Contamination characteristics, source apportionment, and health risk assessment of heavy metals in agricultural soil in the Hexi Corridor. *CATENA, 191*, 104573.

Wang, H., Mi, X., Li, Y., & Zhan, S. (2020b). 3D graphene-based macrostructures for water treatment. *Advanced Materials, 32*, 1806843.

Wang, J., & Ellsworth, M. (2009). Graphene aerogels. *ECS Transactions, 19*, 241.

Wang, W., Gong, Q., Chen, Z., Wang, W. D., Huang, Q., Song, S., Chen, J., & Wang, X. (2019a). Adsorption and competition investigation of phenolic compounds on the solid-liquid interface of three-dimensional foam-like graphene oxide. *Chemical Engineering Journal, 378*, 122085.

Wang, X., Gu, X., Lin, D., Dong, F., & Wan, X. (2007). Treatment of acid rose dye containing wastewater by ozonizing–biological aerated filter. *Dyes and Pigments, 74*, 736–740.

Wang, X., Li, R., Liu, J., Chen, R., Zhang, H., Liu, Q., Li, Z., & Wang, J. (2017). Melamine modified graphene hydrogels for the removal of uranium (VI) from aqueous solution. *New Journal of Chemistry, 41*, 10899–10907.

Wang, X., Lu, M., Wang, H., Pei, Y., Rao, H., & Du, X. (2015). Three-dimensional graphene aerogels–mesoporous silica

frameworks for superior adsorption capability of phenols. *Separation and Purification Technology, 153*, 7–13.

Wang, Y., Hu, X., Liu, Y., Li, Y., Lan, T., Wang, C., Liu, Y., Yuan, D., Cao, X., & He, H. (2021). Assembly of three-dimensional ultralight poly (amidoxime)/graphene oxide nanoribbons aerogel for efficient removal of uranium (VI) from water samples. *Science of the Total Environment, 765*, 142686.

Wang, Y., Xie, W., Liu, H., & Gu, H. (2020c). Hyperelastic magnetic reduced graphene oxide three-dimensional framework with superb oil and organic solvent adsorption capability. *Advanced Composites and Hybrid Materials, 3*, 473–484.

Wang, Y., Zhang, P., Liu, C. F., & Huang, C. Z. (2013). A facile and green method to fabricate graphene-based multifunctional hydrogels for miniature-scale water purification. *RSC Advances, 3*, 9240–9246.

Wang, Z., Zhang, J., Hu, B., Yu, J., Wang, J., & Guo, X. (2019b). Graphene/Fe3O4 nanocomposite for effective removal of ten triazole fungicides from water solution: Tebuconazole as an example for investigation of the adsorption mechanism by experimental and molecular docking study. *Journal of the Taiwan Institute of Chemical Engineers, 95*, 635–642.

Wei, C., Xiang, C., Ren, E., Cui, C., Zhou, M., Xiao, H., Jiang, S., Yao, G., Shen, H., & Guo, R. (2020). Synthesis of 3D lotus biochar/reduced graphene oxide aerogel as a green adsorbent for Cr (VI). *Materials Chemistry and Physics, 253*, 123271.

Wong, L. Y., Lau, S. Y., Pan, S., & Lam, M. K. (2022). 3D graphene-based adsorbents: Synthesis, proportional analysis and potential applications in oil elimination. *Chemosphere, 287*, 132129.

Worsley, M. A., Satcher, J. H., Jr., & Baumann, T. F. (2008). Synthesis and characterization of monolithic carbon aerogel nanocomposites containing double-walled carbon nanotubes. *Langmuir, 24*, 9763–9766.

Wu, S., Zhang, K., Wang, X., Jia, Y., Sun, B., Luo, T., Meng, F., Jin, Z., Lin, D., & Shen, W. (2015). Enhanced adsorption of cadmium ions by 3D sulfonated reduced graphene oxide. *Chemical Engineering Journal, 262*, 1292–1302.

Xiao, J., Lv, W., Song, Y., & Zheng, Q. (2018). Graphene/nanofiber aerogels: Performance regulation towards multiple applications in dye adsorption and oil/water separation. *Chemical Engineering Journal, 338*, 202–210.

Xiao, J., Lv, W., Xie, Z., Song, Y., & Zheng, Q. (2017). L-cysteine-reduced graphene oxide/poly (vinyl alcohol) ultralight aerogel as a broad-spectrum adsorbent for anionic and cationic dyes. *Journal of Materials Science, 52*, 5807–5821.

Xu, Y., & Shi, G. (2011). Assembly of chemically modified graphene: methods and applications. *Journal of Materials Chemistry, 21*, 3311–3323.

Xu, J., Cao, Z., Zhang, Y., Yuan, Z., Lou, Z., Xu, X., & Wang, X. (2018a). A review of functionalized carbon nanotubes and graphene for heavy metal adsorption from water: Preparation, application, and mechanism. *Chemosphere, 195*, 351–364.

Xu, Y., Wu, Q., Sun, Y., Bai, H., & Shi, G. (2010). Three-dimensional self-assembly of graphene oxide and DNA into multifunctional hydrogels. *ACS Nano, 4*(12), 7358–7362.

Xu, Z., Zhou, H., Tan, S., Jiang, X., Wu, W., Shi, J., & Chen, P. (2018b). Ultralight super-hydrophobic carbon aerogels based on cellulose nanofibers/poly (vinyl alcohol)/graphene oxide (CNFs/PVA/GO) for highly effective oil–water separation. *Beilstein Journal of Nanotechnology, 9*, 508–519.

Yan, X., Hu, W., Guo, J., Cai, Huang, L., Xiong, Y., & Tan, S. (2016). Easily separated a novel rGO-MMT three-dimensional aerogel with good adsorption and recyclable property. *ChemistrySelect, 1*, 5828–5837.

Yang, Q., Lu, L., Xu, Q., Tang, S., & Yu, Y. (2021). Using post-graphene 2D materials to detect and remove pesticides: Recent advances and future recommendations. *Bulletin of Environmental Contamination and Toxicology, 107*, 185–193.

Yang, X., Li, Y., Du, Q., Sun, J., Chen, L., Hu, S., Wang, Z., Xia, Y., & Xia, L. (2015). Highly effective removal of basic fuchsin from aqueous solutions by anionic polyacrylamide/graphene oxide aerogels. *Journal of Colloid and Interface Science, 453*, 107–114.

Yap, P. L., Auyoong, Y. L., Hassan, K., Farivar, F., Tran, D. N., Ma, J., & Losic, D. (2020). Multithiol functionalized graphene bio-sponge via photoinitiated thiol-ene click chemistry for efficient heavy metal ions adsorption. *Chemical Engineering Journal, 395*, 124965.

Yap, P. L., Nine, M. J., Hassan, K., Tung, T. T., Tran, D. N., & Losic, D. (2021). Graphene-based sorbents for multi-pollutants removal in water: A review of recent progress. *Advanced Functional Materials, 31*, 2007356.

Yoon, S.-M., Choi, W. M., Baik, H., Shin, H.-J., Song, I., Kwon, M.-S., Bae, J. J., Kim, H., Lee, Y. H., & Choi, J.-Y. (2012). Synthesis of multilayer graphene balls by carbon segregation from nickel nanoparticles. *ACS Nano, 6*, 6803–6811.

Yousefi, N., Lu, X., Elimelech, M., & Tufenkji, N. (2019). Environmental performance of graphene-based 3D macrostructures. *Nature Nanotechnology, 14*, 107–119.

Yu, B., Xu, J., Liu, J.-H., Yang, S.-T., Luo, J., Zhou, Q., Wan, J., Liao, R., Wang, H., & Liu, Y. (2013). Adsorption behavior of copper ions on graphene oxide–chitosan aerogel. *Journal of Environmental Chemical Engineering, 1*, 1044–1050.

Yu, H., Zhu, J., Ren, H., & Liu, S. (2019). Facile Synthesis of Graphene-Based Aerogels and Their Applications for Adsorption of Heavy Metal Ions. *International Journal of Nanoscience, 18*, 1850019.

Zarbin, A. J., & Oliveira, M. M. (2013). Nanoestruturas de carbono (nanotubos, grafeno): Quo Vadis? *Química Nova, 36*, 1533–1539.

Zhan, W., Gao, L., Fu, X., Siyal, S. H., Sui, G., & Yang, X. (2019). Green synthesis of amino-functionalized carbon nanotube-graphene hybrid aerogels for high performance heavy metal ions removal. *Applied Surface Science, 467*, 1122–1133.

Zhang, C., Wang, W., Duan, A., Zeng, G., Huang, D., Lai, C., Tan, X., Cheng, M., Wang, R., & Zhou, C. (2019). Adsorption behavior of engineered carbons and carbon nanomaterials for metal endocrine disruptors:

Experiments and theoretical calculation. *Chemosphere, 222*, 184–194.

Zhang, C., Zhang, R. Z., Ma, Y. Q., Guan, W. B., Wu, X. L., Liu, X., Li, H., Du, Y. L., & Pan, C. P. (2015a). Preparation of cellulose/graphene composite and its applications for triazine pesticides adsorption from water. *ACS Sustainable Chemistry & Engineering, 3*, 396–405.

Zhang, J., Wang, K., Guo, S., Wang, S., Liang, Z., Chen, Z., Fu, J., & Xu, Q. (2014). One-step carbonization synthesis of hollow carbon nanococoons with multimodal pores and their enhanced electrochemical performance for supercapacitors. *ACS Applied Materials & Interfaces, 6*, 2192–2198.

Zhang, L. Y., Zhang, W., Zhou, Z., & Li, C. M. (2016). γ-Fe_2O_3 nanocrystals-anchored macro/meso-porous graphene as a highly efficient adsorbent toward removal of methylene blue. *Journal of Colloid and Interface Science, 476*, 200–205.

Zhang, M., Gao, B., Cao, X., & Yang, L. (2013). Synthesis of a multifunctional graphene–carbon nanotube aerogel and its strong adsorption of lead from aqueous solution. *RSC Advances, 3*, 21099–21105.

Zhang, X., Liu, D., Yang, L., Zhou, L., & You, T. (2015b). Self-assembled three-dimensional graphene-based materials for dye adsorption and catalysis. *Journal of Materials Chemistry A, 3*, 10031–10037.

Zhang, Y., Cui, W., An, W., Liu, L., Liang, Y., & Zhu, Y. (2018a). Combination of photoelectrocatalysis and adsorption for removal of bisphenol A over TiO2-graphene hydrogel with 3D network structure. *Applied Catalysis b: Environmental, 221*, 36–46.

Zhang, Y., Yan, X., Yan, Y., Chen, D., Huang, L., Zhang, J., Ke, Y., & Tan, S. (2018b). The utilization of a three-dimensional reduced graphene oxide and montmorillonite composite aerogel as a multifunctional agent for wastewater treatment. *Rsc Advances, 8*, 4239–4248.

Zhao, L., Dong, P., Xie, J., Li, J., Wu, L., Yang, S.-T., & Luo, J. (2013). Porous graphene oxide–chitosan aerogel for tetracycline removal. *Materials Research Express, 1*, 015601.

Zheng, X., Xiong, X., Yang, J., Chen, D., Jian, R., & Lin, L. (2018). A strong and compressible three dimensional graphene/polyurushiol composite for efficient water cleanup. *Chemical Engineering Journal, 333*, 153–161.

Zhou, F., Feng, X., Yu, J., & Jiang, X. (2018). High performance of 3D porous graphene/lignin/sodium alginate composite for adsorption of Cd (II) and Pb (II). *Environmental Science and Pollution Research, 25*, 15651–15661.

Zhou, F., Yu, J., & Jiang, X. (2017). 3D porous graphene synthesised using different hydrothermal treatment times for the removal of lead ions from an aqueous solution. *Micro & Nano Letters, 12*, 308–311.

Zhou, J., Pei, Z., Li, N., Han, S., Li, Y., Chen, Q., & Sui, Z. (2022). Synthesis of 3D graphene/MnO_2 nanocomposites with hierarchically porous structure for water purification. *Journal of Porous Materials, 9*, 11–23.

Zhuang, Y., Yu, F., Ma, J., & Chen, J. (2016). Facile synthesis of three-dimensional graphene–soy protein aerogel composites for tetracycline adsorption. *Desalination and Water Treatment, 57*, 9510–9519.

Zhuang, Y.-T., Zhang, X., Wang, D.-H., Yu, Y.-L., & Wang, J.-H. (2018). Three-dimensional molybdenum disulfide/graphene hydrogel with tunable heterointerfaces for high selective Hg (II) scavenging. *Journal of Colloid and Interface Science, 514*, 715–722.